A Control Strategy for a V2G- Aggregator for Microgrid Regulation

BY

RANA SAQIB SAEED

01-244172-051

SUPERVISED BY

DR. ASAD WAQAR

Session - 2017 -2019

A Thesis submitted to the Department of Electrical Engineering

Bahria University, Islamabad

in partial fulfillment of the requirement for the degree of MS(EE)

CERTIFICATE

We accept the work contained in this report as a confirmation to the required standard for the partial fulfillment of the degree of MS (EE).

_____	_____
Head of Department	Supervisor
_____	_____
Internal Examiner	External Examiner

DEDICATION

I dedicate this thesis to my Mother Mrs. Samina Saeed who always encouraged and supported me. Her utmost support, countless prayers and blessings have always got me through. Without her belief in me, my success would have been far-fetched.

DECLARATION OF AUTHORSHIP

The substance of this thesis is the original work of the author and due references and acknowledgements have been made, where necessary, to the work of others. No part of this thesis has been already accepted for any degree and is not being currently submitted in candidature of any degree.

_____

(Student Signature)

Rana Saqib Saeed
01-244172-051

ACKNOWLEDGMENTS

First of all I would like to thank my supervisor, Dr. Asad Waqar, who always supported and advised me during my MS studies especially during my research work. I am also thankful to my mentor, Dr. Muhammad Najam ul Islam, who encouraged me to register in MS studies.

I am also grateful to my teachers Dr. Shahid Khan, Dr. Imtiaz Alam and Engr. Muhammad Ali Waqar. I am grateful to my brother and sisters who always encouraged me a lot. My wife and my children were always there to support me.

ABSTRACT

The power system is a very complex and sensitive to sudden change in load, line tripping, generator problem and islanding of grid. These conditions create voltage, current and frequency transients on the utility grid. The second issue is the overloading of the distribution system in which the distribution system is overstressed and increase the losses of the distribution lines and distribution transformer. In these situations, the protection system will operate and the continuity of the service will disturb the distribution system due to load shedding. According to these difficulties, the stability and service continuity of the distribution system is a challenging task.

In this research, Electric Vehicles Batteries are used for overcoming the discontinuity of service, overloading and transient conditions of the distribution system due to their rapid response, efficient control and minimum cost. In this research, introduce a two-way power delivery in which the regulation of charging and discharging of Electric Vehicle Batteries has been introduced to overcome the overloading, line tripping and transient conditions of the distribution system. When power will deliver from utility grid to Electric Vehicles Batteries then the charging current of Electric Vehicles Batteries will be controlled according to the distribution load and protect the distribution transformer and distribution lines to overloading. When the secondary load of the distribution transformer will increase the charging current of the Electric Vehicles Batteries will be decreased by using the charging station controller and protect the distribution transformer to overloading. When the load connected to the secondary side of the distribution transformer will increase again then the charging current of the Electric Vehicles Batteries will be zero and the battery charging will be stopped. When the load connected to the secondary side of the distribution transformer will increase to a specific limit then Electric Vehicles Batteries will start to discharging and provide the power to distribution loads and protect the distribution transformer and distribution lines to overloading without load shedding. When the secondary load of the distribution transformer will decrease, then batteries charging current will increase again and Electric Vehicles Batteries charge to its full rating capacity.

When the abnormal condition occurs in the utility grid, in this condition utility grid switch to islanding mode then Electric Vehicles Batteries behave as a distributed energy source and deliver power to the grid thus increasing the stability of the utility grid in islanding condition. In both overloading and islanding conditions, the charging and discharging of Electric Vehicles Batteries will be controlled and protect the distribution system to overloading and transients without any extra expense.

For this purpose, PI controllers, Fuzzy Logic controllers, and Fuzzy Logic-based PI controllers are used to improve the stability of the grid network during overloading and transient response using Grid to Vehicle (G2V) and Vehicle to Grid (V2G) technologies. This proposed controllers have been simulated in MATLAB/SIMULINK and tested on reference distribution systems. Experimental outcomes illustrate that the proposed controllers successfully stabilize the grid during overloading and transients. Experimental outcomes also illustrate that the Fuzzy Logic controllers provide the better response as compare to PI controllers for stabilizing the grid during overloading and transient conditions.

TABLE OF CONTENTS

ABBREVIATIONS

VSC: Voltage Source Converter

G2V: Grid to Vehicle

V2G: Vehicle to Grid

D-STATCOM: Distributed Static Compensator

PI: Proportional Integrator

EVs: Electric Vehicles

SOC: State of charge

Chapter 1

Introduction

1. INTRODUCTION

Electric Vehicle Batteries (EVs) are cheaper and best response in power systems and used for distributed energy resources in distribution systems. Batteries of electric vehicle are used for providing power to grid for management of load, regulation of frequency, compensation of voltages and resolution of stability. In a power system, stability of the system is a challenging task, in which the small-signal stability, voltage stability, and transient-stability. The most challenging task in all of the above is Transient-stability.

1.1 Thesis Background

In this research, a two -way delivery of power from the grid to electric vehicles (G2V) and vehicle to grid (V2G) is presented. When utility grid is working in normal condition then power will deliver from the grid to electric vehicles(G2V), and when irregular condition appear on utility grid then electric power will deliver from electric vehicles battery (EVs) to grid (G2V).

In this research, voltage source converters (VSC) are introduced for controlling two-way power deliver for load management, voltage sag reduction, frequency regulation and resolving stability issues in the microgrid.

A utility grid of 30MVA, 600 voltages connected to the 420 Volt electric vehicles by using voltages source bi-directional converters. In normal operation bi-directional converter behave as a rectifier and converts the AC power to DC and maintains 500 voltages at the DC load line by using the reference parameters from the slack bus B1 of the system. The battery will be charged with its normal ratings by using the charging station controller which will be based on buck converter and PI controller and fuzzy logic controllers. This charging controller converts 500V DC into 450V DC by using the PI controller and Fuzzy Logic controller and charge the battery at its full rating capacity.

In this case of G2V when the load of the system increases then the charging of the battery of the electric vehicle will be controlled by the charging station controller and battery charging will be reduced.

In case of islanding of utility grid, electric vehicles (EVs) batteries work as a source and maintain the 500 DC voltage at DC load line by using discharging station controller which will be based on boost converter and PI controller and Fuzzy Logic controller. During this period bi-directional converter works as an inverter and invert 500V DC into 240V AC with the help of voltage source converter. Voltage source converter used the reference point from the slack bus B1 and provides the power to the grid and takes up the load of the system. In this case, power will deliver from electric vehicles battery to grid and battery will be discharged.

A second important part of this research is compression between PI and Fuzzy Logic controllers.

In the first case, Six PI controllers are used for ensuring the transient stability of the grid, by utilizing G2V and V2G technology. The First PI controller is used for DC voltage regulation, the second PI controller is used for Iq regulation, the third PI controller is used for Id regulation, the fourth PI controller is used for charging control of electric vehicles battery, Fifth and Sixth PI controllers are used for electric vehicle battery discharging.

In the second case, the first PI controller is tuned by Fuzzy Logic controller which will regulate 500 DC voltages at the DC load line, second and third controllers are PI controllers which are used for regulating the Iq and Id, fourth PI controller is swapped by Fuzzy Logic controller which will be used to control the charging of electric vehicles batteries. The fifth and sixth PI controllers are replaced by Fuzzy Logic controllers which are used for controlling the discharging of electric vehicles batteries.

1.2 Problem Description

In this research, two-way power deliver is introduced for improving transient stability, load management, and voltage regulation during V2G and G2V. For the first case, in normal condition when grid working in its normal condition, small load is connected to grid then voltages source converter working as a rectifier and electric vehicle battery is charged at its full rating capacity. When the load is increased at a specific level then state of charge (SOC) of electric vehicle batteries will be reduced. When the load is increased again then state of charge (SOC) of electric vehicles batteries will reduce again. For the 2nd case when an abnormal condition occurs on the utility power grid and grid come to islanded condition then electric

vehicles batteries discharge to the grid through bi-directional power converter and power delivered from the electric vehicles batteries to the grid for providing active power to grid.

The distribution transformer is used for step down the voltage from 600 AC voltages to 240 AC voltages in case of G2V. Four loads (Two loads Load 1 and load 2 are connected before the Transformer and two Loads Load 3 and load 4 are connected after the transformer), the bi-directional converter is connected at the secondary side of the transformer. Bi-directional converter is a universal bridge which will be based on IGBT/Diodes and received the gate signal from the voltages source converter and converts 240 AC voltages into 500 DC voltages and charge the batteries by using charging station controller which will based on buck converter and control the charging current of electric vehicles batteries by using PI and Fuzzy Logic controller.

In case of islanding of utility grid, the bi-directional converter converts 500V DC into 240V AC in this case distribution transformer step up 240 AC voltage into 600 AC voltages. Load 1 and load 2 are connected at the 600 AC voltages side and load-3 is connected at 240 AC voltages side of the transformer. In this case, power will deliver from the battery to grid and discharging controller maintains 500 DC voltages at the DC load line by using a boost converter by using a PI controller and Fuzzy Logic controller.

Chapter 2

Literature Review

2 LITERATURE REVIEW

In this chapter, the study of various research papers is presented. Many researchers discussed the problem of load sharing procedures for distributed generation units coupled with a Micro-grid [1]. In this research, a load sharing methodology is introduced for non-conventional power resources for voltages and frequency regulation to maintaining the power at the grid for grid-connected and autonomous modes. For this purpose, power electronics converters are introduced for interfacing the combination of the renewable energy resources and storage systems for improving the reliability and flexibility of the utility grid. This is done by sharing the active and reactive power in a grid which is operated in islanding modes. Feeder power losses and line impedance voltages drops are minimized by the power at the point of common coupling by sharing active and reactive power. For this purpose, droop control is utilized for sharing the active and reactive power to the grid.

In modeling of battery energy storage systems (BESS) projects [2] is required for designing and implementation of power conversation systems for automatic power conversion and fast controlling response for a generation, transmission and distribution of electric energy. This paper also concerns about the peak load demand reduction, grid frequency regulation, leveling and smoothing of renewable energy, power quality and reliability for the end user in case of grid-connected and islanding modes. On the base of grid code requirement battery energy storage system send a request to the grid for power delivery and stability.

From the literature review for distribution systems, an AC Microgrid allows to deliver AC power to the grid for grid supporting during normal and abnormal conditions in case of islanding or faulty conditions for increasing the reliability and performance of the utility grid is discussed [3]. By increasing the penetration of the integration of the distributed energy resources generators to utility grids with high controlling power processors based on power electronics converters for communication and controlling purpose. In paper [3] carries out the overview of the microgrid structures and controlling methods for different hierarchical controlling levels. In paper [3] a detailed study of the operation process and controlling methods of different power converters belonging to microgrids has been done. The study is mainly based on the grid forming, grid

feeding, and grid supporting power converters. This paper also analyzes the hierarchical control schemes of the microgrids based on primary and secondary controls for minimizing operation cost and controllability of the microgrids.

Different methods have been used for transient stability by different authors. There are various applications of the microgrid. The system design and the control methods based on the application and the characteristic of stability in a microgrid. In [4] explain the types of transient stability in microgrids. It is known from the literature review, the stability of the system investigated by many authors in recent past time, and they focus on a particular aspect of the stability of the systems. By depending on the controlling parameters, network parameters and types of the microgrids stability aspect discussed in [4] by using voltage source converters interfacing with source integration. The stability of microgrids mainly depends on the controlling topology of the voltage source converters. Others parameters, micro-sources, storages systems, protection schemes, and compensation can play a vital part in the stability of the system. Small signal stability, Dynamic stability with the power electronics distributed generators (DGs) with double-fed induction motors and general stability issues with voltage source converters by using supplementary control are proposed in previous papers to improve previous work. The stability of microgrids in islanding and transient stability after large disturbances analysis with possible contingencies, micro-sources, current limiting and spinning reserve for reactive supports are discussed in recent papers. In research paper [5] discuss various reasons of stability issues in various categories of microgrids to improve system stability, by using different control loops.
In past research papers, many authors discussed the issue of the V2G microgrid for transient stability improvement [5]. In the current situation of the world stability of the grid is a challenging task with high integration of renewable energy resources and electric vehicles battery. This integration would require proper coordination between various electric vehicle battery charging and discharging to the utility grid. Coordination between electric vehicles battery and grid is a relay on the individual state of charge of battery and present grid condition according to load demand. On the base of the state of charge of the electric vehicle battery and grid condition required for grid stability. In the high penetration of electric vehicles, batteries to grid (V2G) technology explore where a large amount of energy of electric vehicles battery can be supplied back to the grid for many purposes with highly controlled fashion. In V2G

technology electric vehicles battery used as a distributed energy source. In this past research paper [5] distribution system of a town is used for meeting peak load demand and voltage regulation by using electric vehicles EVs batteries.

Vehicles to the grid (V2G) is a scheme in which electric vehicle battery communicates to the utility grid to provide power to the grid for compensating voltage regulation, frequency regulation and smoothing and leveling of renewable energy resources. A grid operator is used for coordinating between battery and grid for utilizing the stored energy of electric vehicles battery to the grid. For this purpose, fleet electric vehicles batteries are used for providing considerable stored energy. V2G technology is used for reducing the stress of electric grid on overloading especially during peak hours.

In recent past years, many researchers discussed the advance controlling techniques for examples droop control, Fuzzy control, Fuzzy Inference systems and adaptive Neuro-Fuzzy control for integration of renewable resources, storage systems and distributed devices for improving the stability of the systems.

Chapter 3

Methodology

3 METHODOLOGY

3.1 Overview of Microgrid Organization

The overview of the system is shown in Figure 1. In which a utility microgrid is connected to distribution transformers with a slack bus B1. Load 1 and load 2 are linked between the transformer and the utility grid. The transformer is connected with bi-directional converters at a point of common coupling with the help of the LC filter. At the point of common coupling, load 3 and load 4 are connected with AC-load line after the transformer.

The bi-directional converter is connected with 420 DC battery use as electric vehicle battery (EV) with the help of charging and discharging station controllers. Charging and discharging controller based on buck and boost converters with the help of PI controller and a Fuzzy Logic controller for charging and discharging of EV battery.

Voltage source converter (VSC) is used for controlling bi-directional two-way power flow from the G2V in normal condition and in abnormal condition power will transfer from V2G in case of islanding of grid.

A current control closed loop is introduced for controlling the charging of electric vehicle battery, which will be based on the secondary current of the distribution transformer. The secondary current of the transformer is fixed at 2000 amperes when the load-3 is connected with the system than charging of electric vehicles battery will be reduced at a specific level by using current control closed loop.

When load 3 and load 4 both are connected with the system then again, the secondary current of the transformer is fixed at 2000 amperes but charging of electric vehicles battery again will be reduced at a specific level by using current control closed loop. In this case with both load 3 and load 4 are connected with the grid then the battery will be discharge instead of charging.

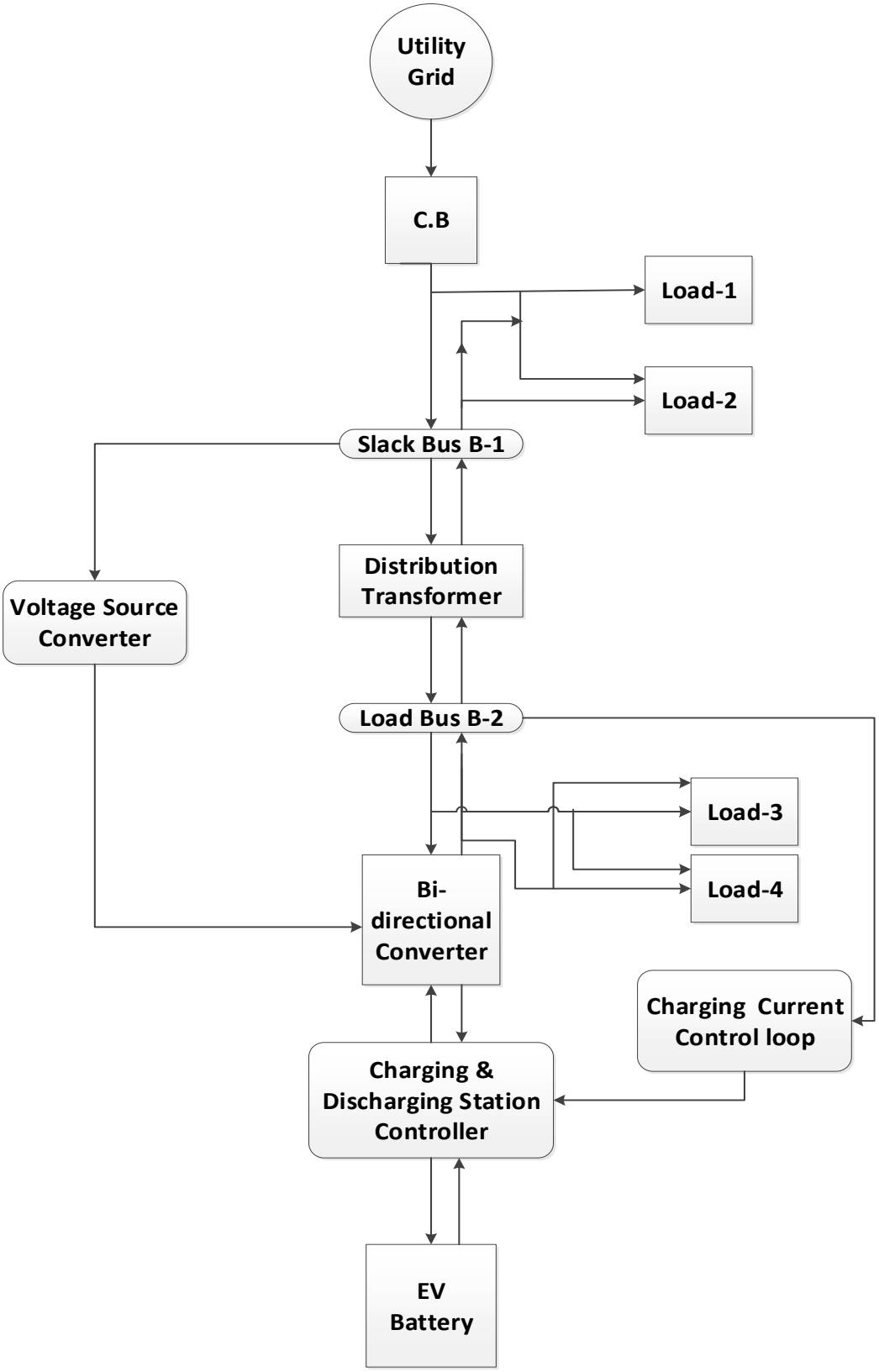

Fig .1 Overview of the Microgrid Organization

3.1.1 Description Of Diagram

A utility grid of 30MVA, 600 voltages connected with a distribution transformer which will step down the voltage at 240 voltages and provide active power to 420volt electric vehicle (EV) battery by using voltages source converter. The converter will provide signal pulses to a universal bridge. In normal operation, this bridge works as a rectifier and changes the AC power to DC power. The voltage source converter maintains 500 voltages at the DC load line from the simulation period 0sec to 0.8sec by using the reference parameters from the slack bus B1 of the system. The battery will be charged until its normal full ratings by using the charging station controller. Charging station controller controls the state of charge of battery by using the Proportional Integral (PI) and Fuzzy Logic controllers(FLC) and charge the battery at its full current rating and electric vehicle battery work as a load.

In this case of the grid to vehicle (G2V) utility grid provides power to Load-1, Load-2, charge the battery at its full rating from 0 sec to 0.2 sec.

From 0.2 sec to 0.4 sec Load 3 (200kw resistive, 200kvar inductive and 300kvar capacitive) will be inter in the system so load increase, then charging station controller bring down the state of charge of the battery will be reduced according to load by using current control loop. The charging station controller controls the state of charge of battery by using a buck converter with the help of a PI and Fuzzy Logic controllers.

From 0.4 sec to 0.6 sec load 3 and load 4 both are connected with the system. In this situation, the battery charging station controller will stop the charging of the battery. In this case, by using current control closed loop with the help of PI and Fuzzy Logic controller battery will be discharged.

From 0.6 sec to 0.8 sec load-4 will disconnect from the system and battery will charge again at its full amperes by using the charging station controller with the help of PI and Fuzzy Logic controller by using a current control closed loop.

In the second case from 0.8 sec to 1.2 sec, the utility grid will switch to islanding mode then electric vehicle (EVs) battery work as a source and discharging station maintain the 500 DC voltage at DC load line by using boost converter with help of PI and Fuzzy Logic controllers.

Discharging station controller has two loops. The outer loop is a voltage control loop and the inner loop is the current control loop.

In this case universal bridge works as an inverter which converts 500V DC into 240V AC by using the voltage source converter(VSC). VSC pick the reference point from slack bus B1 by using PLL Loop and Id ref will be inverted and power will be delivered from EV to the grid. In this case, EV battery will be discharged according to load demand by using the discharging station controller. In this case, bidirectional converter works as inverter and transformer work as a step-up transformer and convert the three-phase 240 AC voltages to 600 AC voltages and provide power to load-1, Load-2, and load-3.

From 0sec to 0.8sec power will transfer from grid to EV battery by using the bi-directional converter as rectifier and VSC maintain the 500 DC voltage at the DC load line and charge the battery. Load-1 and load-2 continuously connected to the system in all simulation time.

From 0.2 sec to 0.4 sec load increase due to load-3, in this situation battery charging will reduced from its full rating to desired load demand and limit the active power of the system and transformer will be protected from overloading by controlling the charging of electric vehicle battery by using current control closed loop and buck converter with the help of PI and Fuzzy Logic Controllers.

From 0.4 sec to 0.6 sec load increase due to load 3 and load 4, in this situation battery charging will reduced, and battery will be start discharging and provide the active power to the system and transformer will be protected from overloading by controlling the discharging of electric vehicle battery by using current control closed loop and buck converter with the help of PI and Fuzzy Logic Controllers.

From 0.6 sec to 0.8 sec load-4 will shed off and charging station will charge the battery to its normal rating by using a current control closed loop and buck converter with the help of PI and Fuzzy Logic Controllers.

From 0.8 sec to 1.2 sec utility grid switch to islanding mode and battery will begin to discharge and provide the power to load-1, load-2 and load-3. In this case, the discharging station controller controls the discharging of electric vehicle EV battery with the help of PI and Fuzzy

Logic controllers, with the help of current and voltage loops. At this stage, power will deliver from battery to grid.

3.2 Major components

Following are the main components:

a) Utility grid
b) Transformer
c) LC Filter
d) Bidirectional converter
e) Voltage source converter
f) Charging station controller
g) Discharging station controller
h) Electric vehicle battery
i) Fuzzy Logic Controller
j) Current Control Loop
k) Loads

3.2.1 Utility Grid

A radial distribution system is shown in the figure below in which Si is total appearance power of the nodes and S_{Li} is the overall power of loads [5].

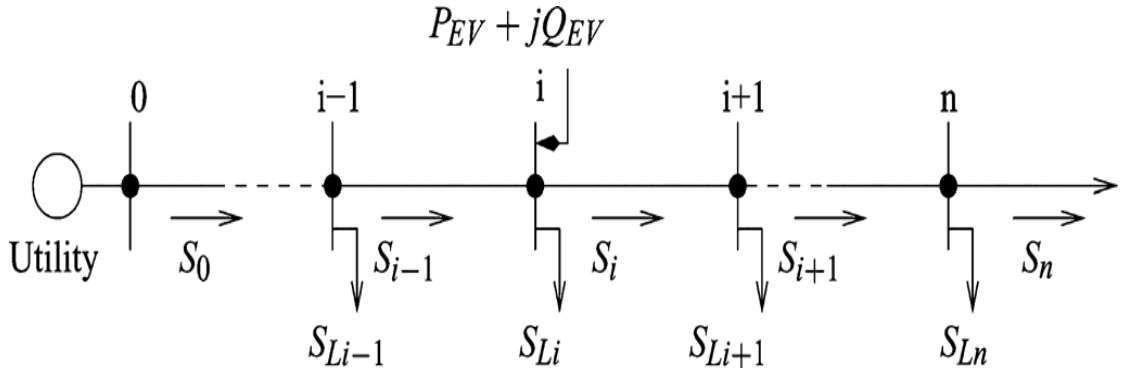

Fig.2. Distribution side of the Grid

The i+1 node voltage shown in Equation-1. Losses of ith nodes are shown in Equation- 2. Similarly ith lines losses are shown in Equation-3 and 4 and Equation-5 shown the voltages delivered by the battery [5].

$$V^2{}_{i+1} = V^2{}_i - 2(P_{iri} + Q_{ixi}) + \left(\frac{P_i{}^2 + Q_i{}^2}{V_i{}^2}\right) r^2{}_i \tag{3.1}$$

$$P_{i+1} = P_i - P_{Li+1} - P_{loss\,i} \tag{3.2a}$$

$$Q_{i+1} = Q_i - Q_{Li+1} - Q_{loss\,i} \tag{3.2b}$$

$$P_{Loss} = \left(\frac{P_i{}^2 + Q_i{}^2}{V_i{}^2}\right) r_i \tag{3.3}$$

$$Q_{Loss} = \left(\frac{P_i{}^2 + Q_i{}^2}{V_i{}^2}\right) x_i \tag{3.4}$$

$$\Delta V_{EV} = \frac{P_{EV} r_i + Q_{EV} x_i}{V_i} \tag{3.5}$$

Equations 3.2, 3.3, 3.4, and 3.5 shows that power delivered of the battery reduce and provide the active power of the system. Electric vehicle battery reduces and provides the active power of the utility grid in islanding condition and transient condition. When high current will flow then battery charging will reduce and protect the transformer to overloading.

3.2.2 Transformer

The transformer is a static device that is used for transmission of electrical energy from source to load and step-up or step-down the voltages at constant power and frequency. Transformer working on Faraday's law of electromagnetic induction and provides electrical energy from one coil to another coil on the base of statically induced E.M.F. Transformer provides electrical energy from one coil to another without an electrical connection but these coils are connected magnetically with each other's. Power transformers are used to step up or step down AC voltages of the power systems on the base of their turns ratio [6]. Turns ratio formula given below.

$$\frac{\boldsymbol{E2}}{\boldsymbol{E1}} = \frac{\boldsymbol{N2}}{\boldsymbol{N1}} \tag{3.6}$$

There are two major types of transformers.

3.2.2.1 Ideal Transformer

Ideal transformers are lossless transformers perfectly couples with high magnetically permeable core and winding with zero Electro Magnetive force. It is only theory based not practically possible.

3.2.2.2 Real Transformer

The real transformer is not a loss-free transformer. Core losses and winding losses are considered in these transformers.

The following losses are considered in a real transformer [6]:

(a) Core Losses

These losses are magnetizing current losses and will consist of

- Hysteresis losses – these losses produced by the nonlinear application of voltages in the core of the transformer.

$$P_h = K_h f {B^{1.6}}_m \ \frac{Watts}{m^3} \tag{3.7}$$

- Eddy current losses_ these losses produce by the Joule heat in core and proportional to the square of the transformer frequency

$$P_e = K_h f^2 t^2 {B^2}_m \ \frac{Watts}{m^3} \tag{3.8}$$

(b) Due to the resistance and leakages reactance of the primary and secondary side of the transformer. Following are losses that occur during this process.

- Joule losses for the resistance of the primary and secondary windings of the transformer.

$$P_c = {I^2}_1 \mathrm{R}_1 + {I^2}_2 \mathrm{R}_2 \ \ Watts \tag{3.9}$$

- Leakage flux due to the core which will pass only in one winding of the transformer and produces reactive impedance in the primary and secondary winding.

$$P_c = I^2{}_1\mathrm{X}_1 \; + \; I^2{}_2\mathrm{X}_2 \;\; Watts \tag{3.10}$$

3.2.3 The equivalent circuit of Ideal Transformer

In the diagram given below show the practical transformer physical behavior by representing an equivalent circuit diagram. Primary and secondary winging joule losses and leakage reactance are shown by the series loop impedance of the circuit [6].

Primary side resistance and reactance are: R_P, X_P

Secondary side resistance and reactance are R_S, X_S.

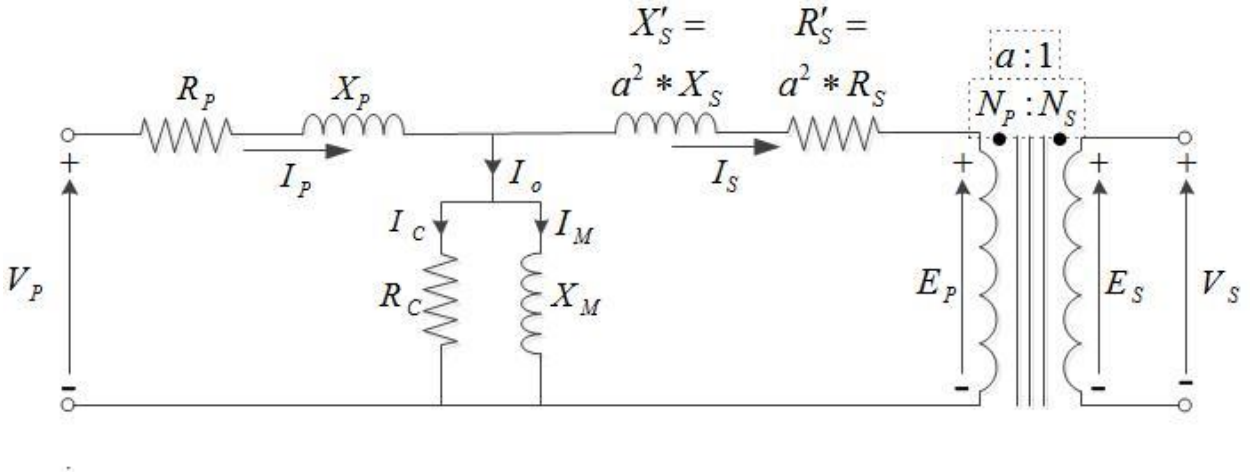

Fig 3 Real Transformer Equivalent Circuit

3.2.4 Transformer EMF Equation

Universal EMF equation of the transformer is given in below E_q where the flux of the core is purely sinusoidal for both sides windings of the transformer, and E are the voltages of the two winding, f is frequency, N number of turns, a is the area of the core in $m^{2,}$ and $\boldsymbol{\phi}_m$ is maximum flux in Web[6].

$$E2 = 4.44 * \mathrm{f} * \text{ø}\mathrm{m} * \mathrm{N2} \quad (3.11)$$

3.3 LC-Filter

3.3.1 Single-Phase Inverter Design

An LC filter circuit based on the inductor and capacitor which will be represented by the capital letters L and C this circuit work as resonance electrical circuit in tuning circuits and storing energy oscillating at the circuit resonance frequency.

An LC circuit accepts that there is no energy loss due to the resistance of the circuit. In a practical implementation of the LC filter circuit always include losses due to resistance but in very small. LC filter circuits are used for oscillating with minimum damping, therefore, the resistance of the circuits as low as possible.

In power systems, LC filters are used for smoothening the current and voltages of the system. Inductor does not allow the abrupt change of current and capacitor does not allow the abrupt change of the voltages so LC filter circuits are used for smoothing the voltages and current of the system.

Due to the uses of the power electronics devices harmonics are produces in the systems so an LC circuit is used for minimizing the harmonics, especially odd harmonics.

Before designing the 3-phase filter first calculated the parameters of single-phase Inverter using PWM technique. For the unique value of the parameters of the LC filter cannot be evaluated based on the output voltage harmonics specification and an additional criterion based on the minimum reactive power of the LC filter is used to specifiy these parameters [7].

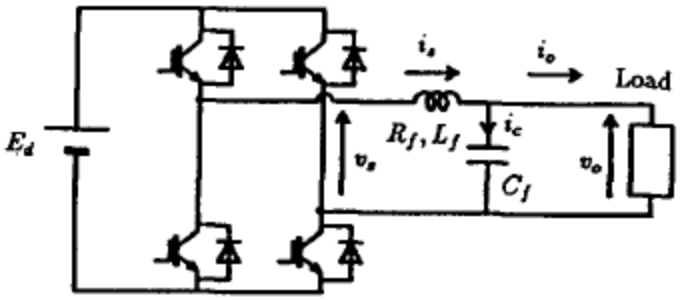

Fig 4 Single Phase PWM Inverter

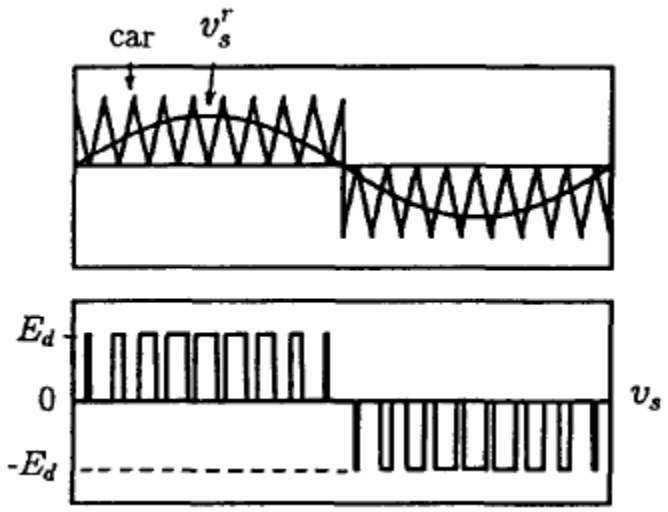

Fig 5. PWM Technique for The Single-Phase Inverter

3.3.2 Inductor Current Harmonic:

From Figure-4 the output voltage equation of the inverter is written as [7].

$$v_s = v_o + R_f i_s + L_f \frac{di_s}{dt} \tag{3.12}$$

The capacitor voltage v_o and inductor current i_s separated into the average (average over one switching cycle) and harmonic (ripple) components,

$$v_o = v_{o-avg} + v_{o-ripp} \tag{3.13}$$

$$i_s = i_{s-avg} + i_{s-ripp} \tag{3.14}$$

Substituting eq-3.13 and 3.14 in equation 3.12

$$v_s = (v_{o-avg} + v_{o-ripp}) + R_f(i_{s-avg} + i_{s-ripp}) + L_f \frac{d(i_{s-avg} + i_{s-ripp})}{dt} \quad (3.15)$$

In a good design filter the value of v_{o-ripp} and $L_f \frac{i_{s-ripp}}{dt}$ are very small as compared to $L_f \frac{di_{s-avg}}{dt}$

So, the ripple component of the filter inductor current is equal to:

$$i_{s-avg} = \frac{1}{Lf} \int (v_s - v_{s-avg}) dt \quad (3.16)$$

Where`

$$v_{s-avg} = v_{o-avg} + R_f i_{s-avg} + L_f \frac{d\, i_{s-avg}}{dt} \quad (3.17)$$

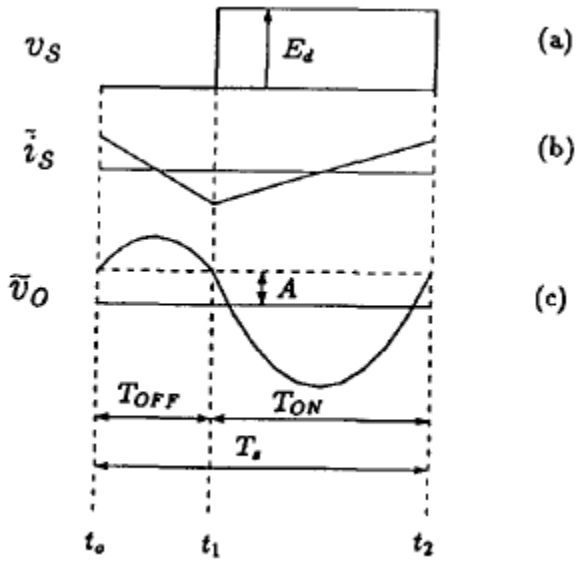

Fig 6. Detailed Output Waveform Over One Switching Period. (a) Inverter Output Voltages (b) Inductor Current Harmonics (c) Capacitor Output Voltage Harmonics

From Figure-6

$$\frac{T_{OFF}}{T_S} = 1 - \alpha \quad (3.18)$$

$$\frac{T_{ON}}{T_S} = \alpha \quad (3.19)$$

$$\alpha = \frac{v_{s-avg}}{E_d} = K\sin\omega_r t \tag{3.20}$$

Where $\omega_r = 2\pi f_r$ here f_r is the fundamental frequency of the output and K is the modulation index. On the base of figure 6a and equation 3.16 the harmonics current deliver in the inductor is:

$$i_{s-ripp} = \frac{E_d}{L_f}\begin{cases} \alpha\,\frac{T_{OFF}}{2} - \alpha(t-t_o), & for\ t_o < t < t_1 \\ -\alpha\,\frac{T_{OFF}}{2} + (1-\alpha)(t-t_1), & for\ t_1 < t < t_2 \end{cases} \tag{3.21}$$

The mean square value of this current harmonic over one switching period

$$(i_{s-ripp})^2 = \frac{1}{T_S}\int_{t_o}^{to\mp T_s}(i_{s-ripp})^2 dt = \left(\frac{E_d}{L_{f*f_s}}\right)^2\left[\frac{\alpha^2-2\alpha^3+\alpha^4}{12}\right] \tag{3.22}$$

Where f_s is switching frequency, so the RMS value of the harmonics over a period of the fundamental output voltages

$$i_{s-ripp-avg} = \sqrt{\left[\frac{1}{2\pi}\int_0^{2\pi}(i_{s-ripp})^2(2\pi * f_r t)\right]} = \frac{E_d}{L_{f*f_s}}\sqrt{\left[\frac{K^2-\frac{16}{3\pi}K^3+\frac{3}{4}K^4}{12}\right]} \tag{3.23}$$

3.3.3 Capacitor Voltage Harmonic:

From figure-4, a filter capacitor current can be determined as [7]:

$$i_c = i_s - i_o \tag{3.24}$$

$$i_s = i_{s-avg} + i_{s-ripp} \tag{3.25}$$

$$i_c = i_{c-avg} + i_{c-ripp} \tag{3.26}$$

Substitute equation.3.24 and equations 3.25 & 3.26 into equation 3.24

$$i_{c-avg} + i_{c-ripp} = i_{s-avg} + i_{s-ripp} - i_{o-avg} - i_{o-ripp} \tag{3.27}$$

Because harmonics of both sides of the equation are the same so

$$i_{c-avg} = i_{s-avg} - i_{o-avg} \tag{3.28}$$

$$i_{c-ripp} = i_{s-ripp} - i_{o-ripp} \tag{3.29}$$

Because filter capacitance is very large so total harmonics current delivered from the Capacitor. Thus, the harmonic components of the current are:

$$i_{c-ripp} = i_{s-ripp} \quad \textit{(approximately)} \tag{3.30}$$

Because ripple current delivers from filter capacitor so, the voltage across capacitor fluctuate around the average, so ripple component of filter capacitor voltages is:

$$V_{0-ripp} = \frac{1}{Cf} \int \left(i_{c-ripp}\right) dt = \frac{1}{Cf} \int \left(i_{cS-ripp}\right) dt \tag{3.31}$$

Substitute 12.10 into 12.20 then

$$v_{0-ripp} = \frac{E_d}{L_f C_f} \begin{cases} A + \alpha T_{OFF} \dfrac{(t-t_o)}{2} - \dfrac{\alpha}{2}(t-t_o)^2, & for\ t_o < t < t_1 \\ A - \alpha T_{OFF} \dfrac{(t-t_2)}{2} + (1-\alpha)\dfrac{(t-t_1)^2}{2}, & for\ t_1 < t < t_2 \end{cases} \tag{3.32}$$

Where A is the average of equation 12.21 over one switching period and A is found by:

$$A = \frac{\alpha^3(1-\alpha) - (1-\alpha)^3}{12\, f_s^{\,2}} \tag{3.33}$$

Figure-6(c) displays the waveform of the filter capacitor harmonics voltages. The mean square value of the filter capacitor harmonics voltages over a complete switching period:

$$(v_{o-ripp})^2 = \frac{1}{T_S} \int_{t_o}^{to+T_s} (v_{o-ripp})^2 dt \tag{3.34}$$

Substituting equation 3.32 in equation 3.34, after performing integration

$$(v_{o-ripp})^2 = \left(\frac{E_d}{L_f\, C_f\, f_s^{\,2}}\right)^2 \left[\frac{\alpha^2 - 5\alpha^4 + 6\alpha^5 - 2\alpha^6}{720}\right] \tag{3.35}$$

The RMS value of the o/p voltage harmonics over a period of the fundamental output voltages can be found by the below-given equation:

$$v_{o-ripp-avg} = \sqrt{\left[\frac{1}{2\pi}\int_0^{2\pi}(v_{o-ripp})^2(2\pi * f_r t)\right]} = \frac{E_d}{L_f C_f {f_s}^2}\sqrt{\left[\frac{K^2-\frac{15}{4}K^4+\frac{64}{5\pi}K^5+\frac{5}{4}K^6}{1440}\right]} \quad (3.36)$$

3.3.4 Design of the output LC Filter

In the designing procedure of the LC filter for fewer losses, size and cost are based on the reactive power. On the base of the minimum reactive power, these parameters are very low and the optimum value of the L and C are achieved [7].

Reactive power can be calculated as:

$$P_r = \omega_r L_f\left({i_{s-avg}}^2 + {i_{s-ripp-avg}}^2\right) + \omega_r C_f\left({v_{o-avg}}^2 + {v_{o-ripp-avg}}^2\right) \quad (3.37)$$

Where $i_{s-avg\ and}\ v_{o-avg}$ is the RMS value of the inductor current and load voltages. Because harmonics components are very small so reactive power approximately equal to the average components.

$$P_r = \omega_r L_f\ {i_{s-avg}}^2 + \omega_r C_f {v_{o-avg}}^2 \quad (3.38)$$

The RMS value of the inductor current is calculated as:

$${i_{s-avg}}^2 = \left[{i_{lr-avg}}^2 + \left({i_{li-avg}}^2 - \omega_r c_f v_{o-avg}\right)^2\right]^{1/2} \quad (3.39)$$

Where $i_{lr-avg}\ \ and\ i_{li-avg}$ are the real and imaginary components of load Current. Substitute equation 3.39 into 3.38.

$$P_r = \omega_r L_f\left[{i_{or-avg}}^2 + \left({i_{oi-avg}}^2 - \omega_r C_f v_{o-avg}\right)^2\right] + + \omega_r C_f {v_{o-avg}}^2 \quad (3.40)$$

From equation 3.36

$$C_f = K\frac{E_d}{L_f {f^2}_s v_{o-ripp-avg}} \quad (3.41)$$

Where K is:

$$K=\left[\frac{k^2-\frac{15}{4}k^{4+}\frac{64}{5\pi}k^5-\frac{5}{4}k^6}{1440}\right]^{1/2} \tag{3.42}$$

Substitute the equation 3.41 into 3.40 the reactive power is calculated by:

$$P_r=\omega_r L_f\left(i_{o-avg}{}^2+\frac{\omega_r{}^2 E_d{}^2 K^2 v_{o-avg}}{L_f f^4{}_s v_{o-avg}{}^2}-\frac{2\omega_r E_d K(i_{oin-avg}*v_{o-avg})}{L_f f^2{}_s v_{o-ripp-avg}}\right)+\frac{\omega_r E_d K\, v_{o-avg}{}^2}{L_f f^2{}_s v_{o-ripp-avg}} \tag{3.43}$$

Where i_{o-avg} is the RMS value of the load current. Minimum reactive power is given by:

$$\frac{\eth P_r}{\eth L_f}=0 \tag{3.44}$$

so, the value of the inductor is calculated by the equation given below:

$$L_f=\frac{V_o-avg}{I_o-avg f_s}\left\{K\frac{E_d}{V_o,av}\left[1+4\pi^2\left(\frac{f_r}{f_s}\right)^2 K\frac{E_d}{V_o-avg}\right]\right\}^{1/2} \tag{3.45}$$

After the calculation of inductor value, the capacitor value would be calculated by the equation 3.46

$$C_f=K\frac{E_d}{L_f f^2{}_s v_{o-ripp-avg}} \tag{3.46}$$

3.3.5 The design procedure of the LC filter:

On behalf of the above analysis design would be divided into these steps:

(a) For the calculation of the modulation index, the output RMS voltages of the inverter are equal to the output RMS voltages of the load. so, the modulation index is [7]:

$$K=\sqrt{2}\frac{V_o-avg}{E_d} \quad (3.47)$$

The result from equation 3.42 is then used to calculate the K.

(b) Then on the base of the $I_o - avg$, $V_o - avg$, f_r and f_s calculate Inductor value from equation 3.45

(c) Then calculate the Capacitor value from equation 3.47

3.4 Second Method For Design Procedure Of The Single-Phase Inverter:

Below Fig 7 &8 shows the single-phase inverter. It is controlled by pulse width modulator [8].

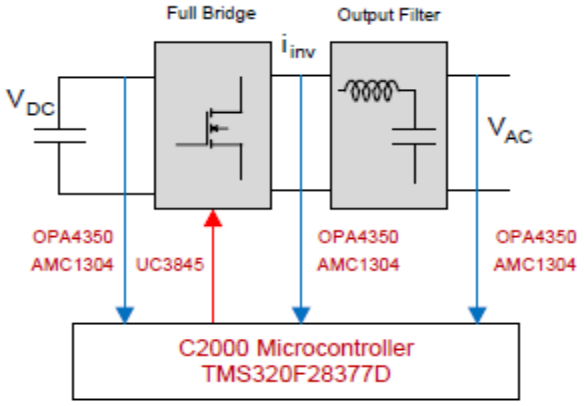

Fig 7. The Typical Single-Phase Inverter

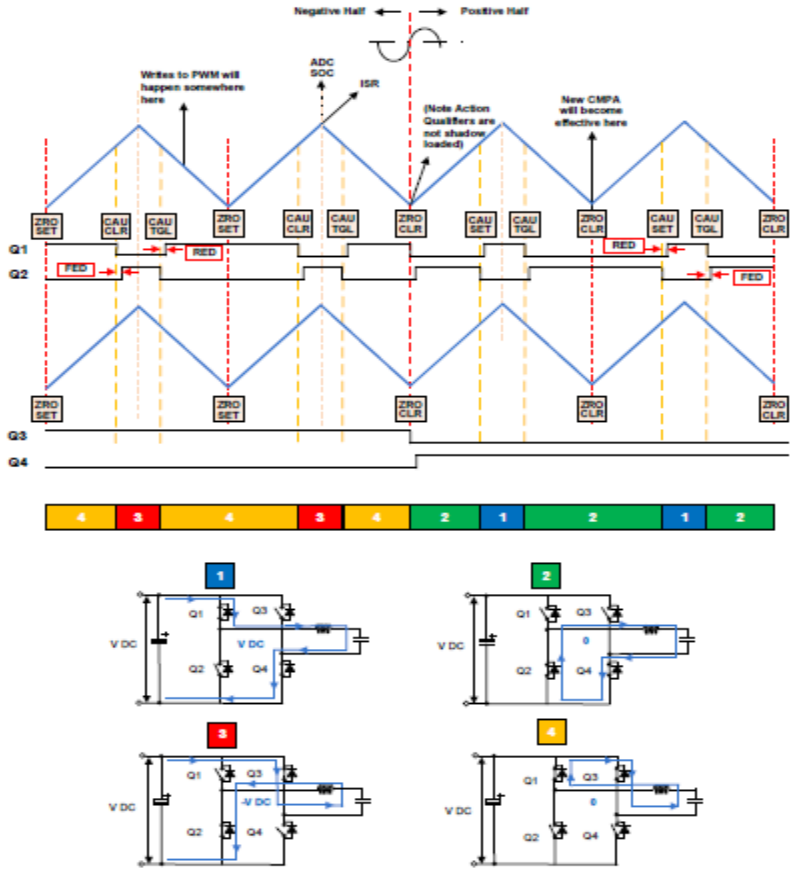

Fig 8. PWM Waveform Generation Using PWM Peripheral Onc2000 MCU

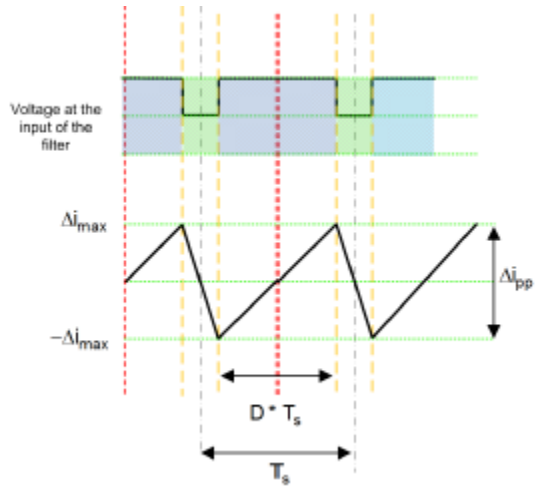

Fig 9. Current Ripple Calculation

In Figure-9 show the one switching cycle waveform of the inverter output voltage VL with regards to inductor current. The voltages across the inductor are given by [8]:

$$V = L_i \, di/dt \tag{3.48}$$

For the full-bridge inverter with an AC output

$$V_{BUS} - V_O = L_i \frac{\Delta i_{pp}}{D \times T_S} \tag{3.49}$$

Where $T_S = \frac{1}{f_{Sw}}$ is the switching period. For rearranging ripple current at any instant in AC waveform given by

$$\Delta i_{pp} = \frac{D * T_S * (V_{BUS} - V_O)}{L_i} \tag{3.50}$$

Assuming the modulation index is m_a , then the duty cycle is:

$$D(\omega t) = m_a \sin \omega t \tag{3.51}$$

The output of the inverter must match the AC voltages so:

$$V_O = V_{DC} D \tag{3.52}$$

$$\Delta i_{pp} = \frac{V_{BUS} * T_S * m_a * \sin(\omega t) \ (\mathrm{I} - m_a \sin(\omega t))}{L_i} \tag{3.53}$$

The find out the modulation index where the maximum ripple is present differentiate the equation 3.53 with regard to time and put it equal to zero

$$\frac{d\Delta i_{pp}}{dt} = \mathrm{K}\{\cos(\omega t)(\mathrm{I} - m_a \sin(\omega t)) - m_a \sin(\omega t) * \cos(\omega t)\} = 0 \tag{3.54}$$

$$\sin(\omega t) = \frac{1}{2m_a} \tag{3.55}$$

When the modulation index for which the ripple is maximum, substitute back in equation 3.53. The inductance value required to tolerate the ripple is given below

$$\Delta i_{pp(max)} = \frac{V_{BUS} * T_S}{4 * L_i} \tag{3.56}$$

$$L_i = \frac{V_{BUS}}{4F_{SW} * \Delta\, i_{pp(max)}} \tag{3.57}$$

3.5 Three Phase Inverter Design

The designing of the output filter for three-phase inverters is based on single phase inverter filter design which will be explained in above and equation 3.12 show the value of the output filter design. For three phase 3 leg bridge inverter with 2 level PWM for star and delta load shown in Figures 9 and 10 [9].

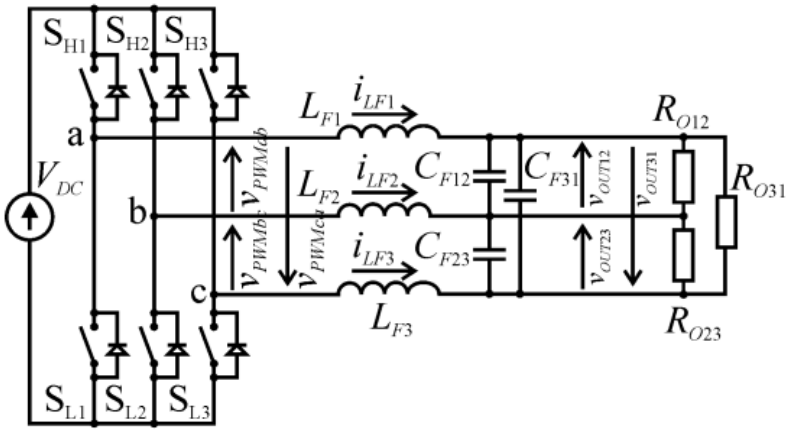

Fig 10. Three phase inverters with delta load.

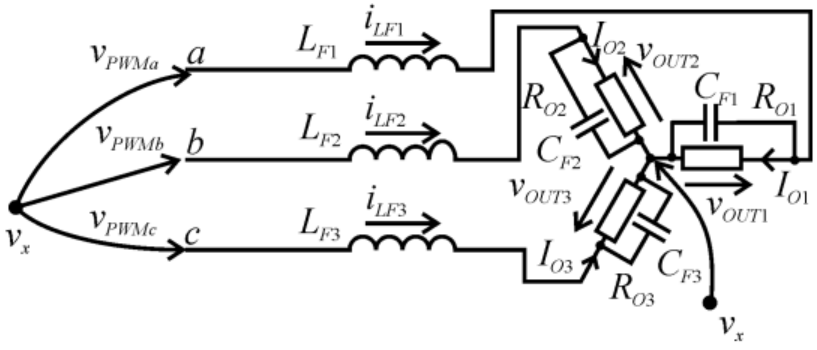

Fig 11. Three Phase Inverters with Star Load

The sequence of the PWM phase to phase changes in six-part($\pi/3$) width of the fundamental period. For a balance, three-phase load analyze line to line voltages. The relation of the line to line voltages is given in equation 3.58 [9].

$$V_{outrk12pp}(\omega_m KT_S\,, M\,)/\left(\sqrt{3}\,MV_{DC}\right) \tag{3.58}$$

$V_{outrk12pp}$ is maximum when M=1.

$$\left.\frac{V_{outrk12pp}(\omega_m KT_S\,, M\,)/2}{\left(\sqrt{3}\,MV_{DC}\right)/2}\right|_{MAX} \leq 3\% \tag{3.59}$$

The equivalent "e" value calculated for $V_{OUTTeh12RMS} \approx V_{OUTeRMS}$

$$\frac{\partial P_{re}}{\partial L_F} \approx\ \omega_m \left(I^2{}_{oe\,RMS} -\ K_{LCe}\frac{1}{f^2{}_c}\frac{1}{f^2{}_{Fe}}\,V^2{}_{OUTe\,RMS}\right) \tag{3.60}$$

The final equation of the L and C for the output filter is given in equation 3.61

$$L_{Fe} \approx \sqrt{k_{LCe}}\ \frac{1}{f_c}\ \frac{V_{OUTeRMS}}{I_{OeRMS}} \quad , \quad C_{Fe} \approx \sqrt{k_{LCe}}\ \frac{1}{f_c}\left(\frac{1}{V_{OUTeRMS}/I_{OeRMS}}\right) \tag{3.61}$$

3.6 Bidirectional Converter as Voltage Source Converter (VSC):

For the improvement of the transient stability of the utility grid which uses G2V and V2G technology, two-way transfer of the power is essential for this reason 3-level and 2-level (IGBT/DIODES) universal bridge is utilized for bi-directional converters.

When the power is transfer from the grid to electric vehicles battery a 3-level universal bridge working as a rectifier and converts 3-phase 240V AC into a 500V DC. The electric vehicle battery is charged by using the charging station controller which will be based on buck converter using a PI and Fuzzy controllers. In this case, Universal Bridge receives a gate signal from a voltage source converter (VSC-1).

In the abnormal condition when grid switching to islanding modes then three-level (IGBT/DIODES) universal bridge work as inverter and converters 500 DC voltages into 240 AC

voltages at this time three-level (IGBT/DIODES) universal bridge receive its gate signal from voltages source converter (VSC). In this case, VSC picks its reference signal from slack-bus (B1), but idref will be inverted. In this case, the battery will be discharged through the discharging controller and power will be transferred from the battery to the grid.

Voltage Source Converter

Power converters are divided into 3 major types Grid-forming, Grid-feeding, and grid-supporting VSC converters. Grid-forming power converters are characterized as an ideal ac voltage source and a very low-output impedance by using the voltage amplitude $E*$ and frequency $\omega*$ of the utility grid with a proper control loop. Grid-feeding power converters made for delivering power to an energized utility grid and characterized as an ideal current source is linked in parallel to the grid with high impedance. For this purpose, $P*$ and $Q*$ represent the active and the reactive powers which delivered to the utility grid. For accurately regulate the active and reactive power to the grid the current source should be perfectly synchronized with ac voltages at the point of connection. Grid-supporting power converters represented by either an ideal ac controlled current source with parallel shunt impedance, or an ideal voltage source in series with link impedance. These converters are used to control their current or voltage for keeping the frequency and voltages of the grid to its desired rating. Grid-forming power converters are executed by using two side by side synchronous controllers working on the *DQ* reference frame. Where amplitude $E*$ and the frequency $\omega*$ to be generated by the power converter at the point of common coupling (PCC). External loop is used for matching the voltages to its reference and internal current loop regulate the current supplied to converters.

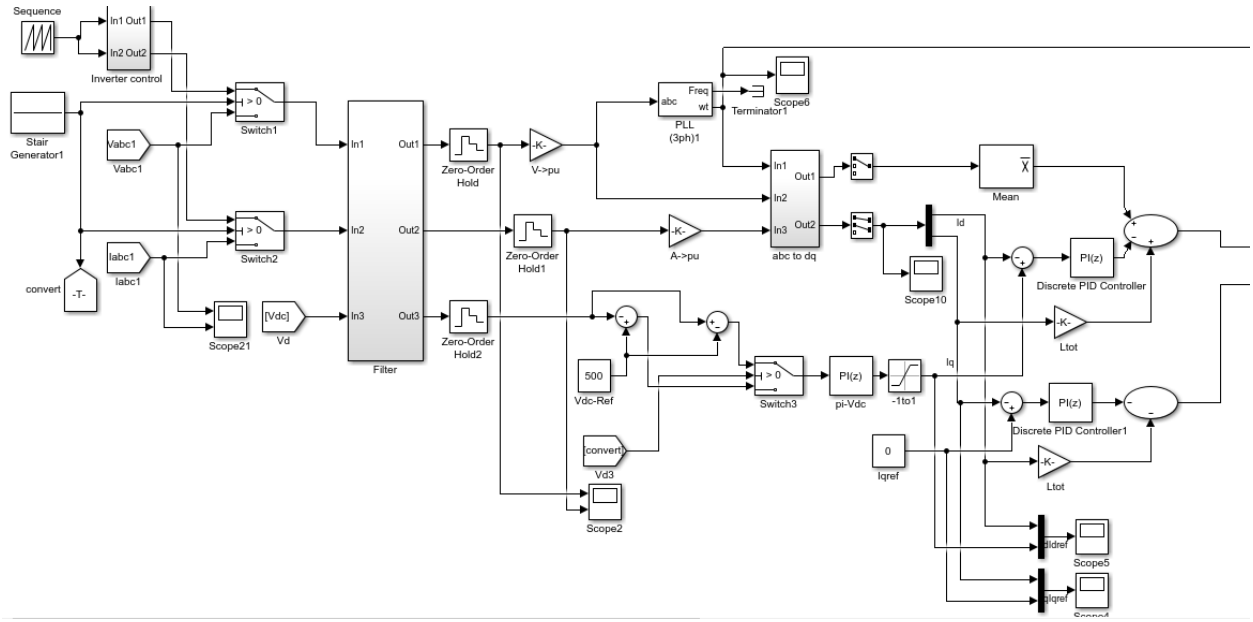

Fig 12a. Voltage Source Converter

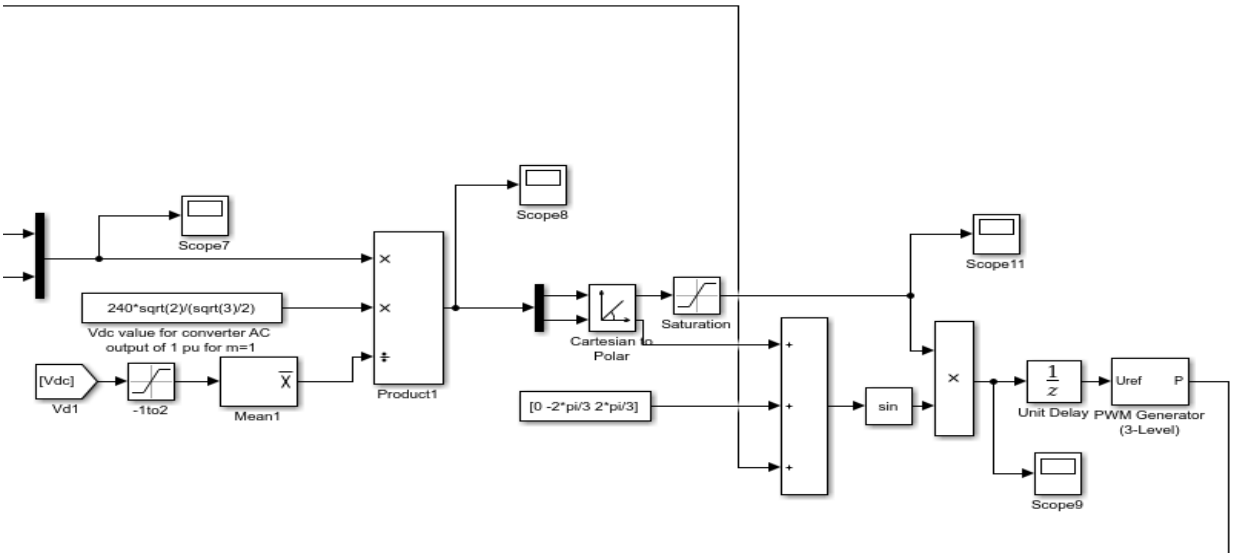

Fig 12b. Control Design of A 3-Phase Grid-Forming Voltage Source Inverter

---

Effect of Droop Control on grid impedance: Droop control loop considered as an ideal voltage control source is associated with line impedance is shown in Figure [14].

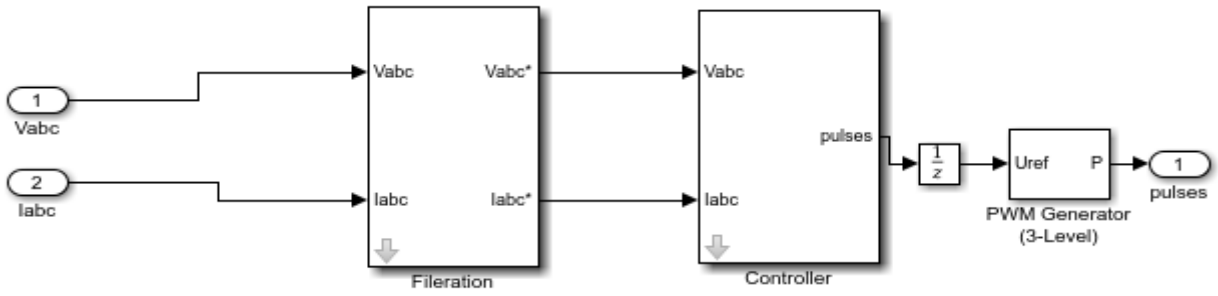

Fig 13. Grid Feeding Power Converter

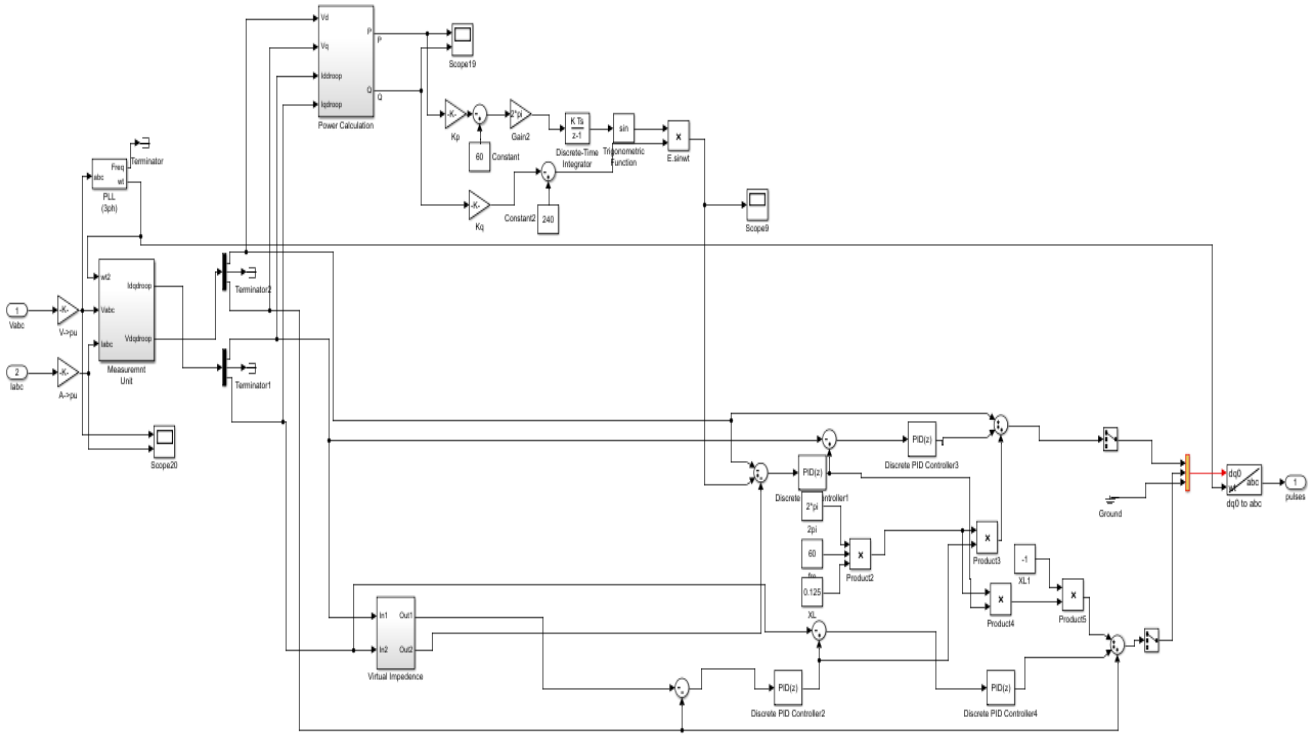

Fig 14. Control Design of 3-Phase Grid-Supporting Power Converters

a) ***Inductive grid****:* In high voltage and low voltage network inductive component of line impedance is higher than resistance, therefore, resistance will be neglected without any error considered, and power angle δ is very small.

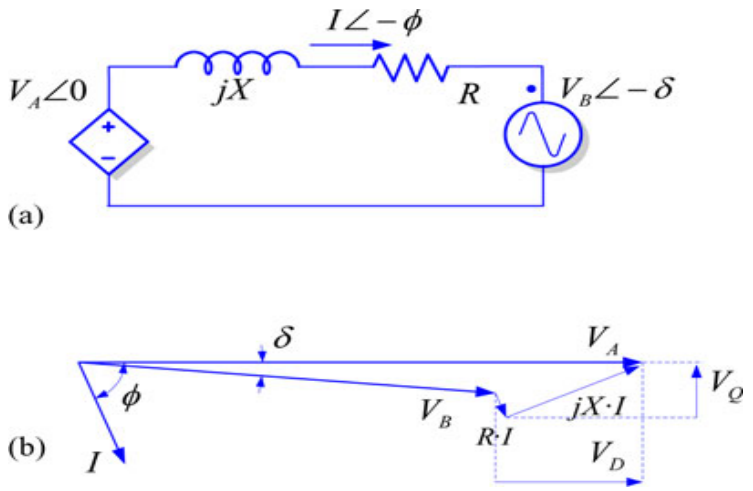

Fig 15. Modeling Of Power In The Distribution Network. (a) Equivalent Circuit. (b) Phasor Diagram.

b) Resistive grid: In case of HV and LV networks the grid impedance is mainly resistive and neglects the inductance of the grid so voltage amplitude is mainly depending on the active power of the grid and frequency is affected by the active power injunction. Droop control characteristics are represented in Figure -16.

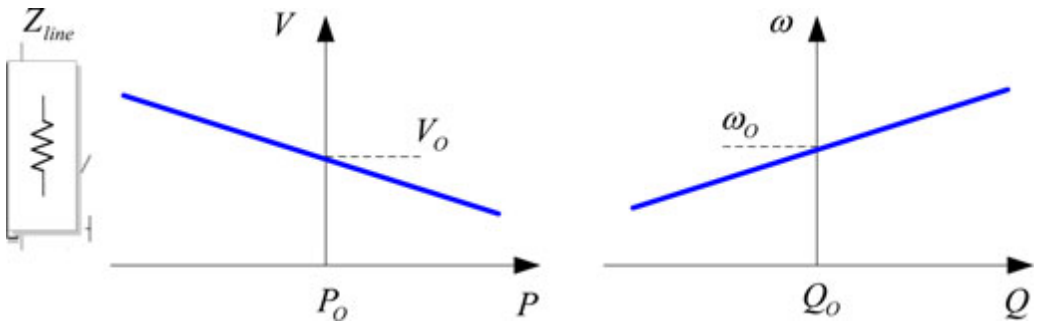

Fig 16. Frequency and voltages droop characteristics for resistive grids for the LV system.

D. Virtual Impedance Control

For the regulation of the voltages and frequency in the MV, the network is controlled by the p/f and q/v droop control using virtual impedance is used for the distribution system is given in the figure below.

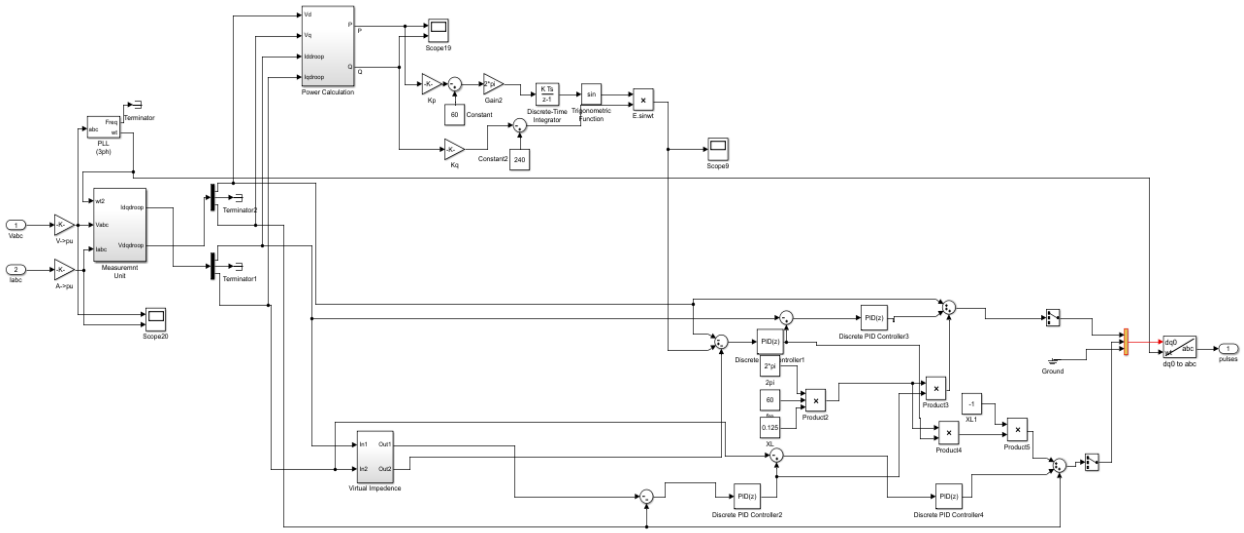

Fig 17. Simulation Diagram the Virtual Output Impedance Loop With *P* And *Q* Droop in the Power. Grid Converter

3.7 Charging Station Controller Using Buck Converter

It is a PI and Fuzzy Logic controller based buck converter which will be utilized to regulating the charging of the electric vehicle's battery. A buck converter is mostly utilized as stepping down the DC voltage at a specific level, by using i/p voltage source, controlled switch S, Diode D, filter inductor L, filter capacitor C, and a load resistor R by using close control loop of the current and PI controller and Fuzzy Logic controller [10].

The converter state in which inductor current never becomes zero for the given time called continuous conduction mode. When the switch is closed the diode is in reverse biased and when the switch is in off condition then diode provides uninterrupted inductor current.

The relation between the input and output voltages and the duty cycle of the switch is shown in Equation 3.62.

$$(V_S - V_O) * DT = -V_O(1 - D)T \tag{3.62}$$

DC voltages transfer function, described by the output to input voltages is given in Equation-3.63

$$MV \equiv V_O/V_S = D \tag{3.63}$$

Equation -3.63 shows that the output voltages is small than the input voltages.

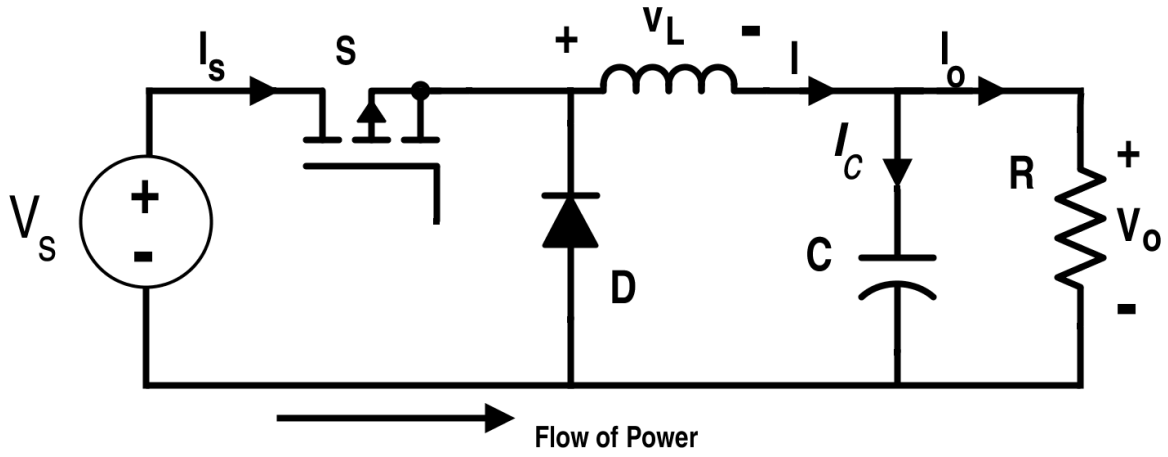

Fig 18. Buck Converter.

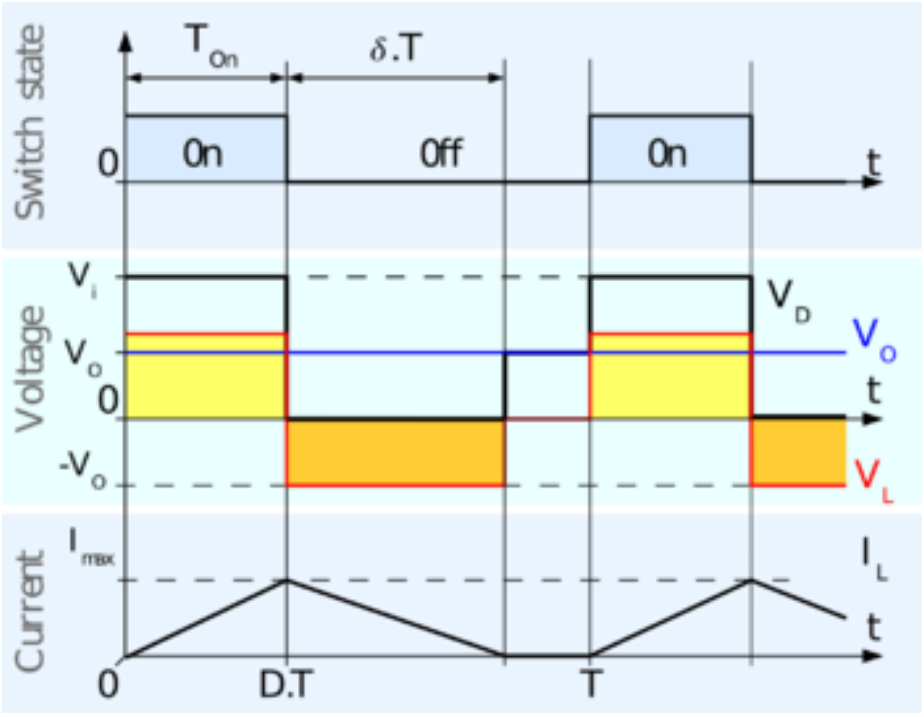

Fig 19. Waveforms of the Buck Converter

According to CCM and DCM, the value of the inductor is determined by Equation 3.64

$$L_b = (1 - D)R/\,2f \tag{3.64}$$

The value of the capacitor depends on the Ic, It causes small ripples across output voltages, for limiting the value of ripple voltages. These values are below a certain value of V_r so capacitor C is always larger than C_{min} and determined by the Equation-3.65.

$$C_{min} = (1 - D)\, VO/8Vr\, Lf\, 2 \qquad (3.65)$$

3.7.1 Discharging Station Controller Using Boost Converter:

Discharging station controller depends on a boost converter by using a PI controller and Fuzzy Logic controller with the voltage and current closed loop. A boost converter is a circuit which is used to stepping up the DC voltages at a specific level. Boost Converters compromised of the DC input voltage source Vs, increase inductor L, controlled switch S Diode D, Capacitor *C*, and load resistance *R*. For CCM is represented in Figure 20(a) and 20(b).

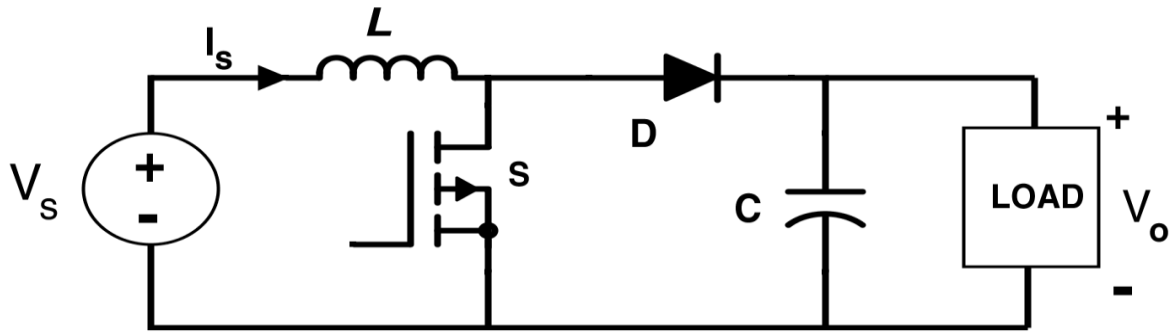

Fig 20a. Boost Converter.

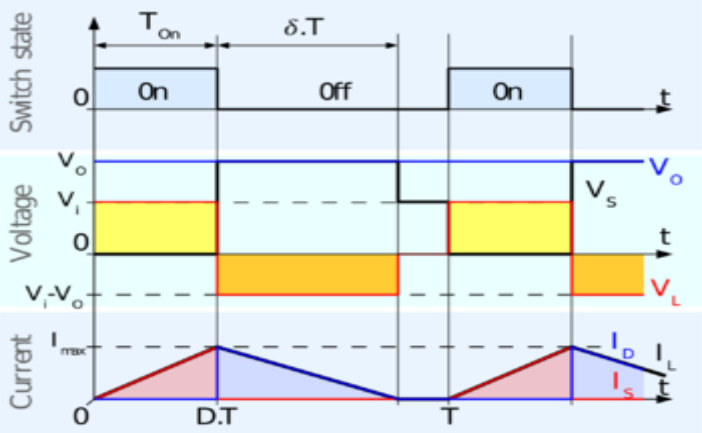

Fig 20b. Waveforms of the Boost Converter

When the switch has closed the current in the inductor current rises smoothly and the diode is in the off state. When the switch is open, boost inductor released to the load through diode and output voltages is greater than the input voltages

Due to the Faraday's law, boost inductor voltages determined by the Equation -3.66.

$$VSDT = (VO - VS)*(1 - D)T \quad (3.66)$$

The boost converters output voltage is larger than the input voltage and boost converter always operates in the CCM for $L > L_b$ where L_b is given by the Equation-3.67.

$$L_b = (1 - D)2DR/2f \quad (3.67)$$

As shown in Figure.20a large capacitor is compulsory to limit the o/p voltage ripples. The capacitor value is determined by Equation -3.68 when ripple voltages Vris given.

$$Cmin = DVO/Vr\ Rf \quad (3.68)$$

3.8 Modeling Of Electric Vehicle Batteries

In this research electric vehicles battery work as a sink in case of G2V and work as a source in case of V2G using a bi-directional converter for supporting the utility grid in case of the transient condition and deliver the active power to the grid for frequency variation, voltage sag reduction and smoothing the renewable energy resources. So bidirectional converter linked with battery at point b [5].

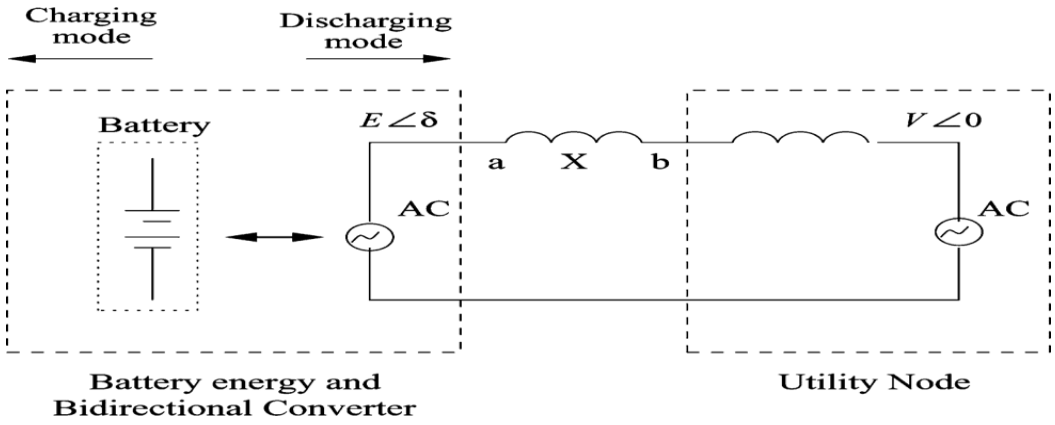

Fig 21. Evs Batteries Used as an Energy Source

Electric vehicles battery consuming and delivering the power to the grid is determined by the Equation-3.69 and current of the battery is determined by the Equation-3.70.

$$S_{EV} = VI \star \tag{3.69}$$

$$I = \frac{E\angle\delta - V\angle 0}{jX} \tag{3.70}$$

In the above equations, E and V are sending end and receiving end voltages of the battery. Equation -3.71 is used to determining the total power of the battery; Equations 3.72 and 3.73 are used to determining the active and reactive power of the battery.

$$S_{EV} = \frac{EVsin(\delta)}{X} + j\frac{E\{E - Vcos(\delta)\}}{X} \tag{3.71}$$

$$P_{EV} = \frac{EVsin(\delta)}{X} \tag{3.72}$$

$$Q = \frac{E\{E - Vcos(\delta)\}}{X} \tag{3.73}$$

3.9 Current Control Closed Loop

For modeling of the current control, a closed loop secondary current of the transformer is used as reference current which will be not exceeded to 2000 amperes. An error is generated for using the secondary using reference 2000 amperes. This error is again comparing with the battery charging current and control charging current of the battery by utilizing PI and Fuzzy Logic controllers at specific rating according to load demand when the load is increased then charging current will decrease using this current control closed loop. When the load is decreased then charging current of the battery will be increased using this current control closed loop using PI and Fuzzy Logic controllers.

3.10 Loads

In this thesis, four distributed loads are used for checking the fluctuations of current, voltages, power and frequency. Load 1 and load 2 are connected for the whole time, load-3 and load-4 connected to check the fluctuation of frequency, current, voltages, and power during peak time.

- LOAD-1: 50W Resistive and 500KVAR Capacitive Load
- Load-2: 500KW Resistive Load
- Load-3: Three phase RLC LOAD (1.50MW resistive, 1.50MVAR inductive and 1.5MVAR Capacitive load)
- Load-4: Three phase RLC LOAD (1.0MW resistive, 1.0MVAR inductive and 1.0MVAR Capacitive load)
- Load-5: 1.25 Ohms
- Load-6: 1.25 Ohms
- Battery: battery is used for the following purposes
- Work as a variable load in a normal condition in case of G2V.
- Work as a source during grid islanding as a source in case of V2G.
- Rating of battery: 10000AH, 420 voltages, the initial state of charge 80%, Battery response time 30 seconds.

Chapter 4

Simulation and Results

4 SIMULATION AND RESULTS

This model is divided into two simulation parts.

4.1 Simulation Model Using PI controllers:

1. The first controller is (PI controller) DC voltage regulating controller (Maintain 500 DC voltage at DC load line in case of G2V and invert 500 DC voltages into 240 AC voltages in case of V2G)
2. The second controller is (PI controller) Id regulating controller (regulate Id in both G2V and V2G cases)
3. The third controller is (PI controller) Iq regulating controller (regulate Iq in both G2V and V2G cases)
4. The fourth controller is (PI controller) charging station controller (regulate the charging current of the battery according to load demand)
5. The fifth controller is (PI controller) discharging station voltage regulating controller (regulate the voltage of outer loop of the discharging station)
6. The sixth controller is (PI controller) discharging station current regulating controller (regulate the current of the inner loop of the discharging station)

4.1.1 First Simulation Model

In this portion of the research discussed the complete simulation model of the system using MATLAB (2017A) Simulink using Discrete Power GUI. A 30MVA, 600 voltages source work as a utility grid and providing the power of 4 ac loads, 2 DC loads and 1 Electric vehicle battery by using the universal bridge with the help of voltage source converter using different controlling techniques.

In normal condition, power will be delivered from the grid to loads and electric vehicles battery for charging. In this case, load demand will be varied and battery charging will be controlled for protecting overloading of the transformer and managing the load demand.

In case of any abnormal event in utility grid, grid switch to islanding modes and power will transfer from electric vehicles battery to grid and battery work as a primary energy source.

Overall Simulation of this project is subdivided into the following major parts:

(1) Utility Grid
(2) VSC
(3) Bi-Directional Converter
(4) Charging Station controller using Buck Converter
(5) Discharging Station controller using Boost Converter
(6) EV Battery
(7) Current Control Closed loop
(8) PI and Fuzzy Logic Controller

4.1.2 Utility Grid

Utility grid having a voltage rating of 600V AC, 60 Hz, 30MVA three phase AC voltage source have been simulated to provide power to four AC loads, two DC loads and one EV battery using voltage source converter, a bidirectional converter, and a 3-phase two winding transformer. 3-phase transformer utilized to step-down 600V into 240V in case of G2V and bidirectional converter work as a rectifier and convert these 240V AC into 500V DC.

In case of V2G when irregular condition appears on utility grid then EV battery work as a source and bidirectional converter work as an inverter and invert 500 V DC into 240V AC and transformer work as a step-up transformer and convert 240 three phase ac voltages into three phases 600 ac voltages.

The parameters of this three phase ac voltages source block are given below:

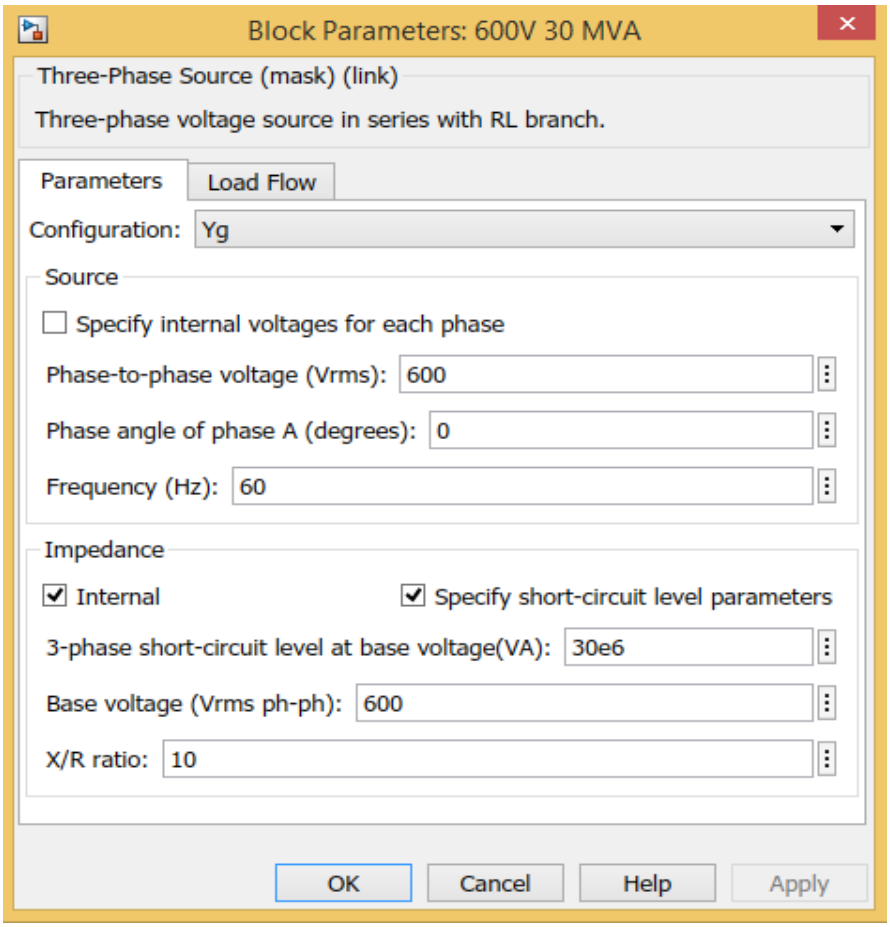

Fig 22a. Block Parameters of the Bridge

4.1.3 Voltage Source Converter

The Simulation figure of voltage source converter VSC is shown in Figure -22b. VSC pick reference parameters of three phase voltages and currents from slack bus-B1 and 500 DC voltages from the DC load line.

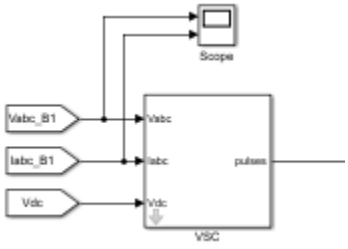

Fig 22b. Block Diagram of VSC

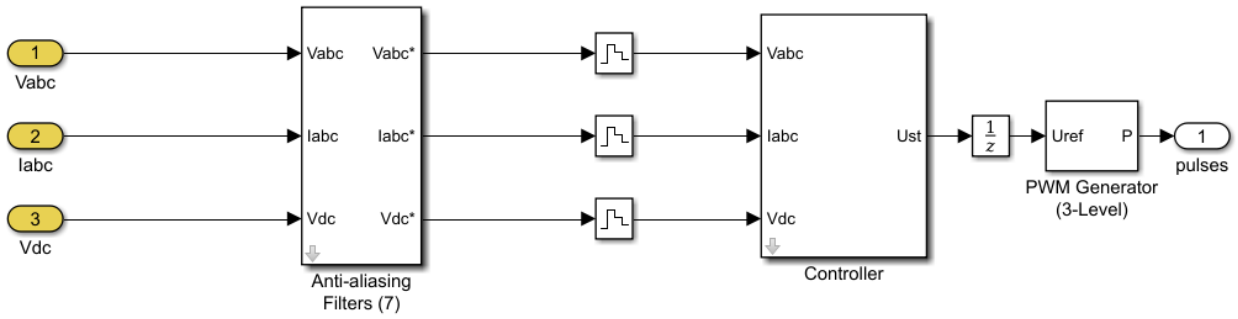

Fig 22c. Block diagram of VSC.

For better requirements 2nd order filters are used for smoothing the system response. From slack bus B-1 Vabc and I_{abc} are receive and convert these into per unit system for computational time reduction. Phase lock loop is used for the providing Wt both inverting and converting cases. DQ frames are used for converting Vabc into vd and vq and I_{abc} to id and iq.

DC regulation is used for the regulating 500 DC voltages using PI controllers for both converter and inverter cases, and provides reference point Idref to id which will be received from DQ frame. Providing Iq_{ref} =0 to iq which is received from the DQ frame. For regulating the id and iq two PI controllers are used for regulating id and iq according to the Idref and Iqref.

The current regulator provides Vd and Vq to cartesian by using Wt from PLL block.

Now Cartesian form converted the input signal into three-phase Vabc in per unit. These three Vabc provide pulses to the bi-directional converter by using three-level (PWM). In Figure-22d show the controller diagram of VSC.

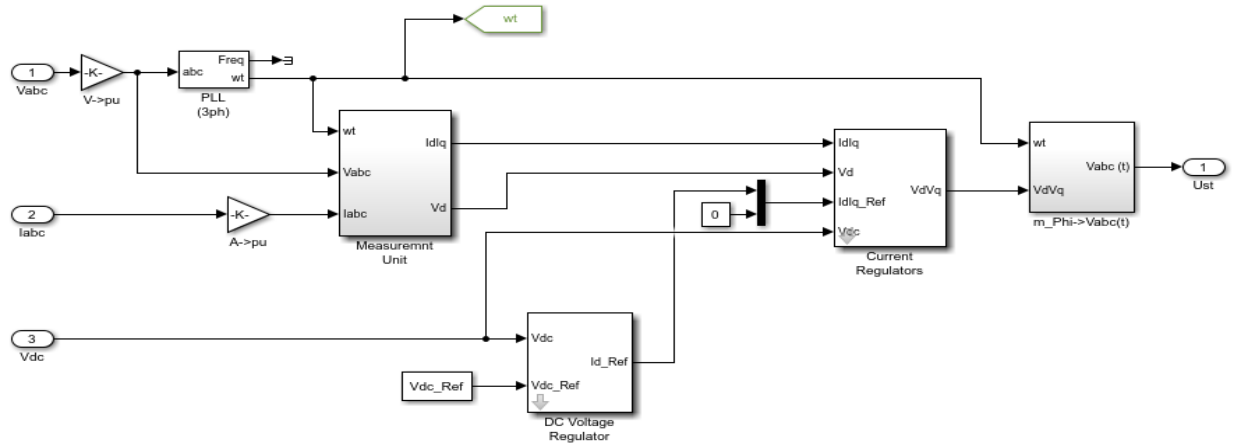

Fig 22d. Block Diagram of the Controller of VSC

Normally when power transfer will occur from grid to loads and electric vehicle battery, VSC pick reference values from slack bus B-1 and gives Idref as positive and Id is negative then universal bridge work as a rectifier and transforms 240V AC into 500V DC. In this situation charging station controller charge the battery at 450 DC voltages.

In the abnormal condition when power will deliver from EV battery to grid, VSC Pick reference parameters from slack bus B-1 but in this case Idref is negative and Id is positive and bidirectional converter work as an inverter and inverts 500V DC into 240V AC. In this situation discharging station controller discharge the battery at its full rating and power will deliver from EV battery to grid. In this case, the discharging controller maintains 500 DC voltages at the DC load line.

In DC voltages regulator block PI controller is used for regulating the DC voltage and responsible for maintaining 500 DC voltages at the DC load line. Simulation diagram of this DC voltages regulator is given in Figure-23 (a) and Figure-23 (b)

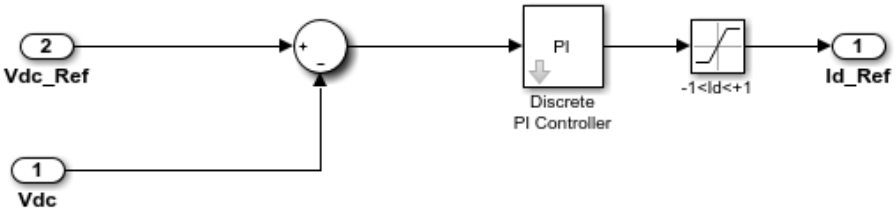

Fig 23a. Diagram of DC Voltages Regulator

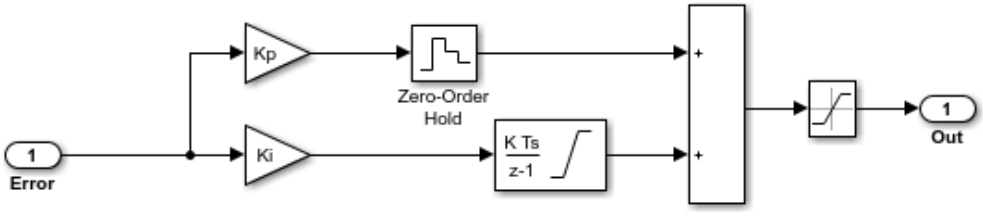

Fig 23b. Diagram of DC Voltages Regulator

In Current Regulator block, two PI controllers are used for regulating the Id and Iq using Idref and Iqref. Idref is provided from DC voltage regulator block and Iq_ref=0. Current regulator

block is responsible for minimizing the error of Id and Iq and provide Vd and Vq to next block. Simulation diagram of this current regulator block is given in Figure-24.

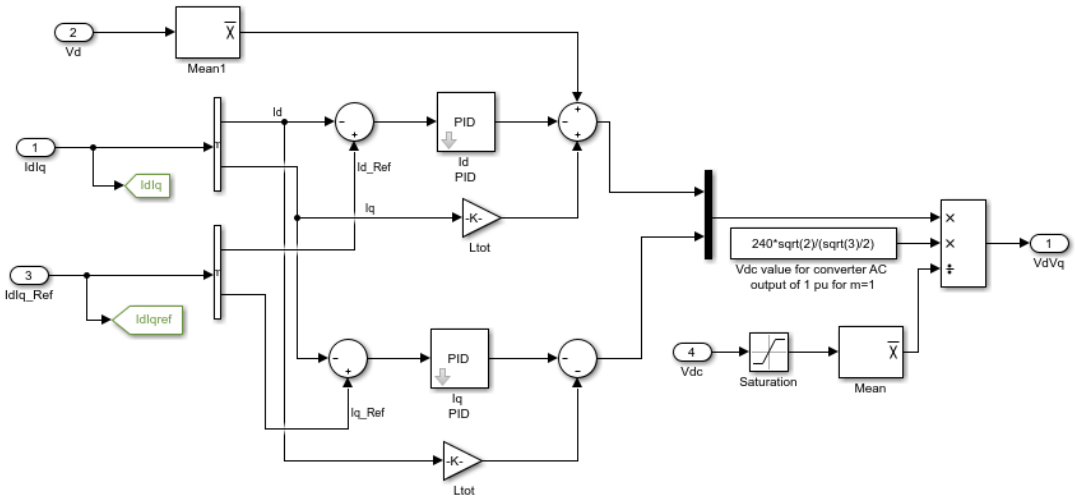

Fig 24. Diagram of Current Regulator Block

In m_Phi->Vabc (t) block convert VdVq into Vabc per unit and provide the signal to three level PWM Generator. The simulation diagram of m_Phi->Vabc (t) block is given in Figure-25.

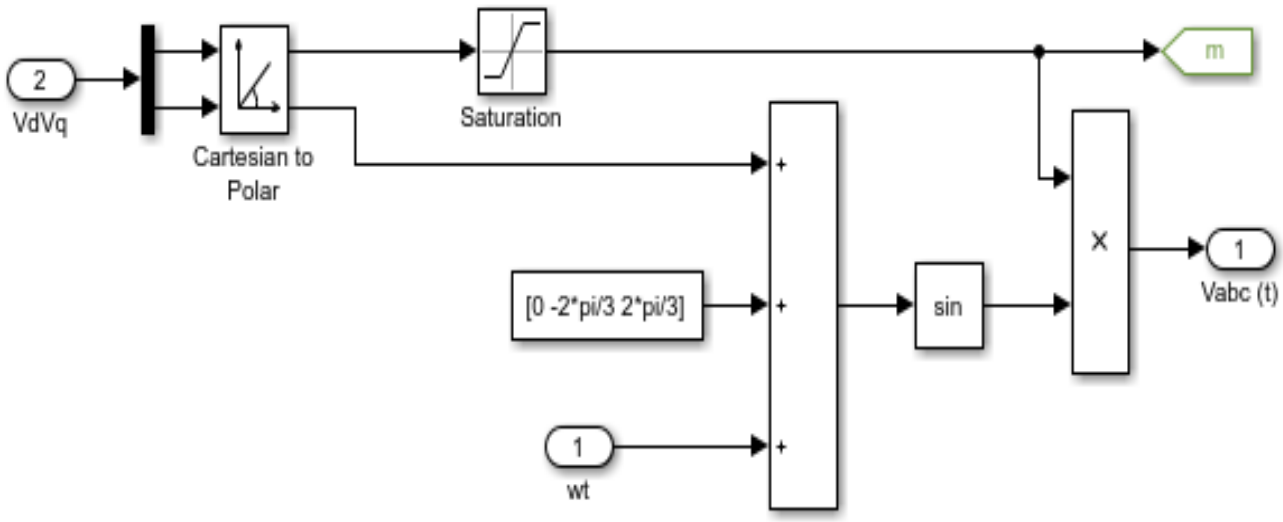

Fig 25. Diagram M_Phi->Vabc (T) Block

4.1.4 Bi-Directional Converter

For improving the transient response of the system G2V and V2G technology is being utilized and bidirectional transfer of the power is essential for this reason 3-level (IGBT/DIODES) universal bridge is utilized for bi-directional converters.

When the power is transfer from the grid to loads and 3-level universal bridge act as a rectifier in electric vehicle and converts three phase 240V AC into a 500V DC and electric vehicle battery is charged by using charging station controller which will be based on buck converter using a PI controller. In this case, the universal bridge receives a gate signal from voltage source converter VSC. In the abnormal condition when grid switching into islanding modes then three-level (IGBT/DIODES) universal bridge work as an inverter and inverts 500V DC into 240V AC using gate signal from voltages source converter VSC. In this case, VSC picks its reference signal from slack-bus (B1), but Idref will be inverted. In this case, the battery will be discharged through the discharging controller and power will transfer from battery to grid.

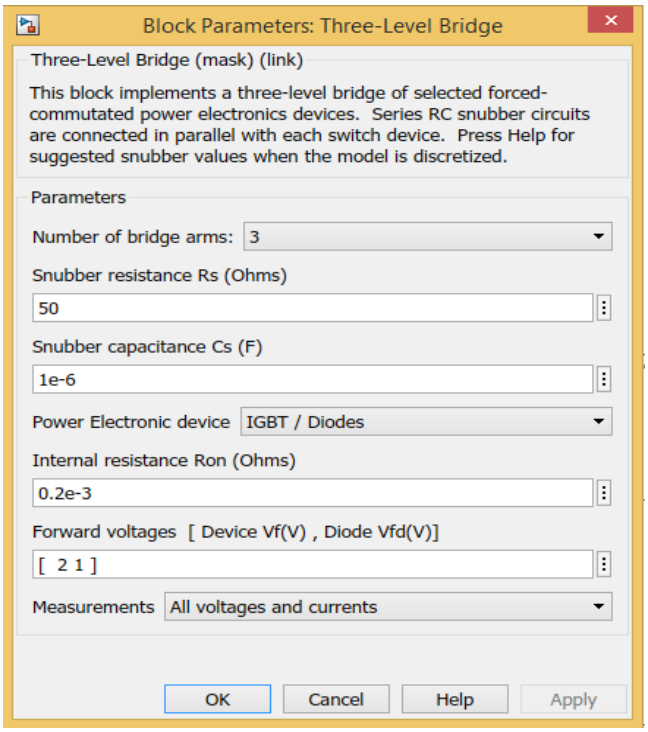

Fig 26. Block Parameters of Three Level Bridge

4.1.5 Charging Station Controller Using Buck Converter

In case of power transfer from G2V, VSC gets reference values from slack bus B-1 and gives Idref as positive and Id is negative then bidirectional converter work as a rectifier and convert 240V AC into 500V DC. In this situation charging station controller charge the battery at its desired value, by using a PI controller current control closed loop and provide the PWM to MOSFET and charge the battery according to the reference point of the charging station controller. Charging station controller uses a current control closed loop and minimizing the error of the current according to demand. Figure-27 shows simulation diagram of the universal bridge, DC load line, charging station controller, discharging station controller, Buck-Boost converter and battery.

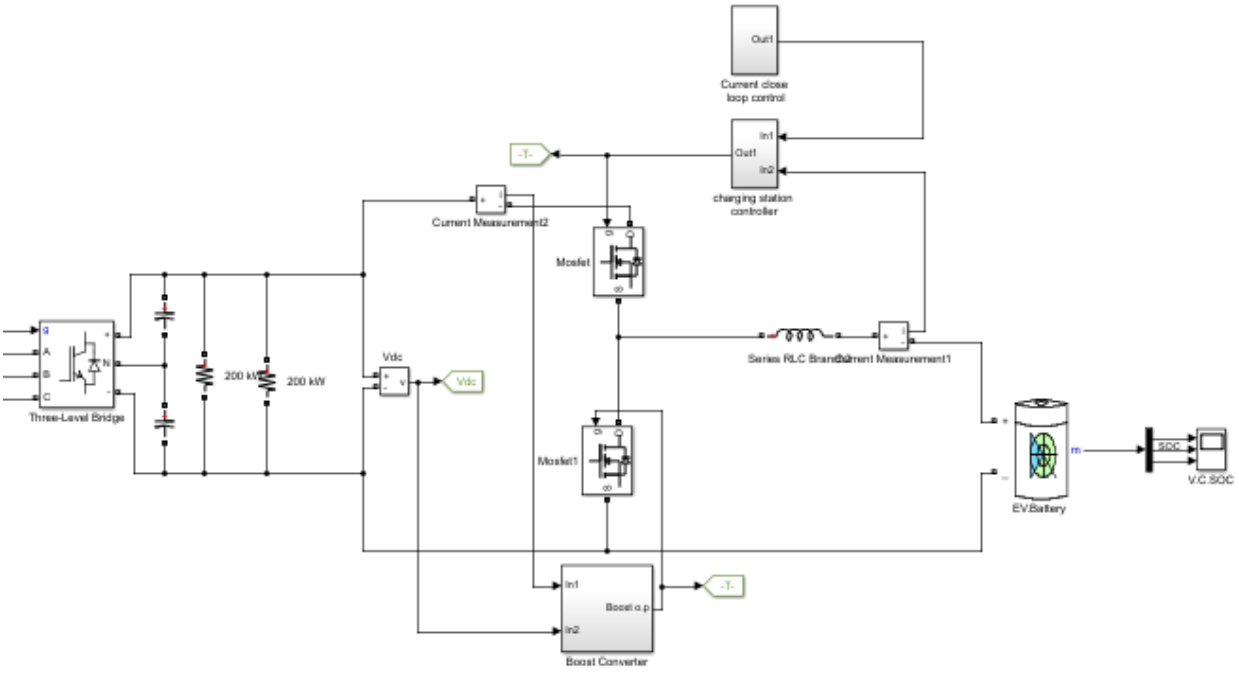

Fig 27. Simulation Diagram of the Charging and Discharging Station Controllers

For modeling of the current control, closed loop secondary current of the transformer is used as reference current which will be not exceeded to 2000 amperes. An error is generated for using the secondary using reference 2000 amperes. This error is again comparing with the battery charging current and control the charging current of the battery using a PI controller at specific rating according to load demand when the load is increased then charging current will decrease

using this current control closed loop. When the load is decreased then charging current of the battery will be increased using this current control closed loop using PI Controller. Simulation diagram of the current control closed loop and the charging station controller are given in figure [28] and figure [29].

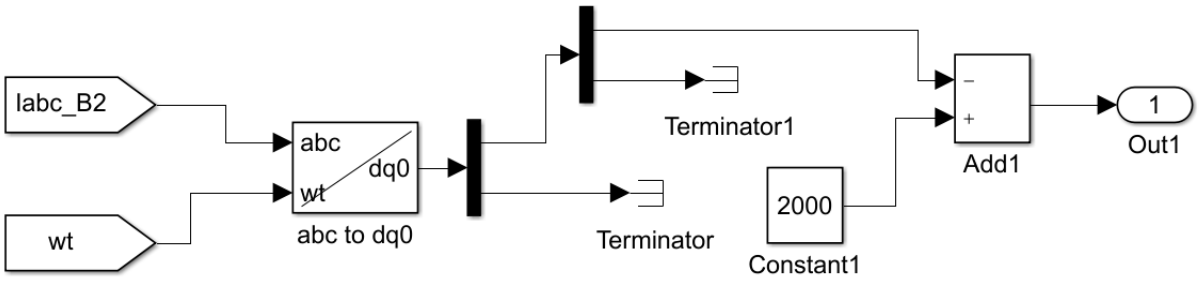

Fig 28. Simulation Diagram of the Current Control Closed Loop

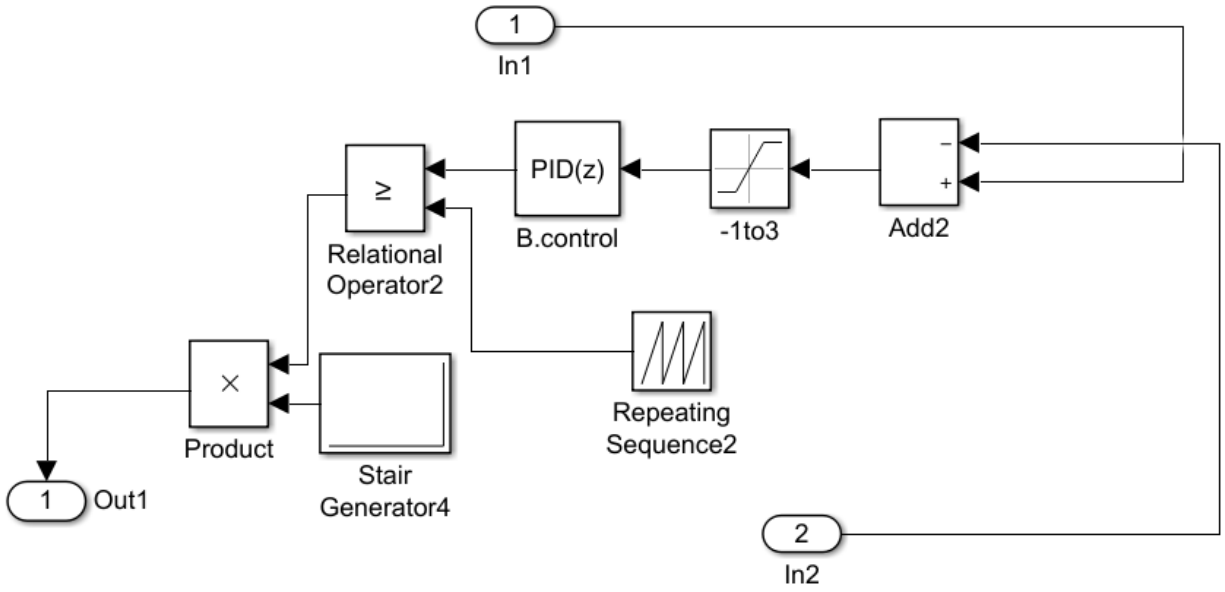

Fig 29. Simulation Diagram of the Charging Station Controller Using PI Controller

4.1.6 Discharging Station controller using a boost converter

In the abnormal condition when power will transfer from the electric vehicle battery to grid, VSC pick reference parameters from slack bus B-1 but in this case, Idref is negative and bidirectional converter acts as inverter and inverts 500V DC into 240V AC. In this situation, dis-charging station controller discharges the battery according to load demand and power will deliver from V2G. In this case, discharging controller maintain 500 DC voltages at the DC load line by using two control loops, the external loop is for voltage control and the internal control loop is for current control and that is achieved using two PI controllers. Discharging station controller provides PWM signal to MOSFET, for maintaining 500 DC voltages at DC lad line. Figure 30 shows the discharging station controller.

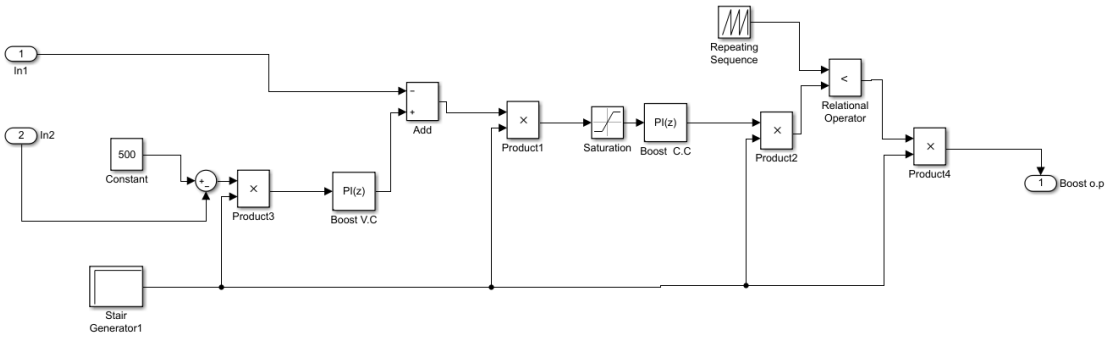

Fig 30. Discharging Station Controller

4.1.7 Eletric Vehicle Battery

In this model Nickel Metal Hydride(NiMH), 420V, 80% SOC, 10000 amperes hours' rated capacity battery is used for 30 seconds response time. In normal operation, the battery works as a load and charge at its desired rating by using charging station controller reference points. In abnormal operation in case of islanding, the battery will be discharged by using discharging controllers and work as a source and delivered power to the utility grid and state of charge of the battery will reduce.

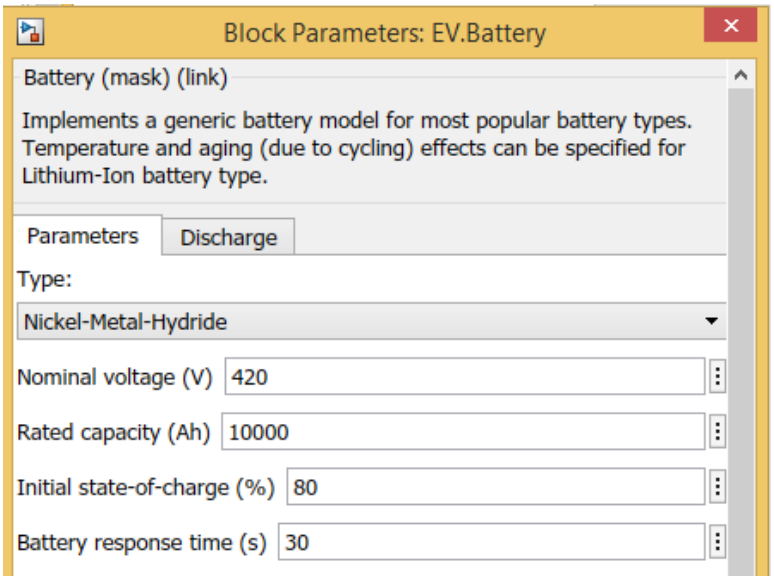

Fig 31. Electric Vehicle Battery Parameters

4.2 Simulation Model Using Fuzzy Controllers:

1. The first controller is (Fuzzy Logic based PI controller) DC voltage regulating controller (Maintain 500 DC voltage at DC load line in case of G2V and invert 500 DC voltages into 240 AC voltages in case of V2G)
2. The second controller is (PI controller) Id regulating controller (regulate Id in both G2V and V2G cases)
3. The third controller is (PI controller) Iq regulating controller (regulate Iq in both G2V and V2G cases)
4. The fourth controller is (Fuzzy Logic controller) charging station controller (regulate the charging current of the battery according to load demand)
5. The fifth controller is (Fuzzy Logic controller) discharging station voltage regulating controller (regulate the voltage of the outer loop of the discharging station)
6. The sixth controller is (Fuzzy Logic controller) discharging station current regulating controller (regulate the current of the inner loop of the discharging station).

4.2.1 Second Simulation Model:

In this model First controller which is a DC voltage regulating controller is tuned by the FLC using Fuzzy Logic rules and control Kp and Ki of the PI controller. Simulation diagram of this controller is shown in Figure-32 (a, b and c).

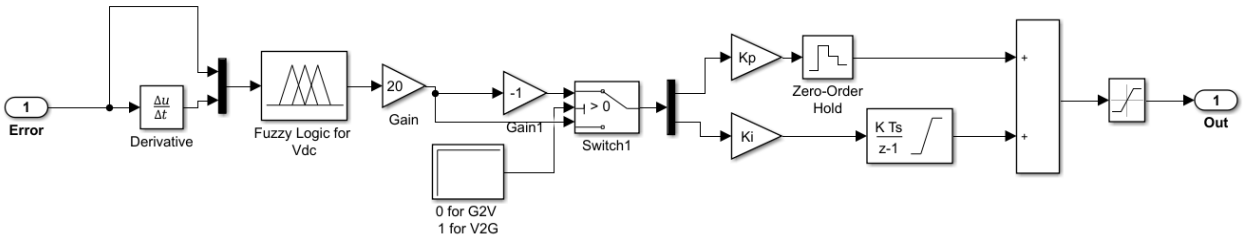

Fig 32a. Diagram of PI-Based Fuzzy Logic DC Voltages Regulator

In the above diagram, the Fuzzy controller has been used to minimize the error of the DC load line voltages. The input of this Fuzzy system is error and derivative of error of DC voltage. Proportional gain (Kp) and Integral gain (Ki) are the output of this PI controller.

Membership functions for inputs and outputs are:

Negative big (NB), Negative medium (NM), Negative small (NS), Zero (ZO), Positive small (PS), Positive medium (PM), Positive big (PB).

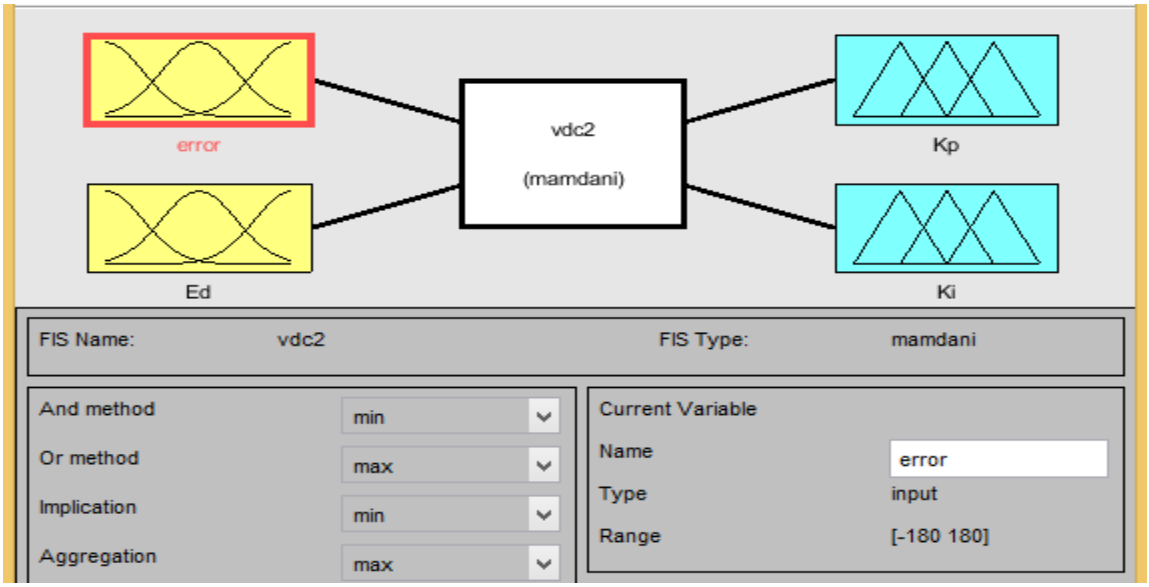

Fig 32b. GUI for V_DC Regulator.

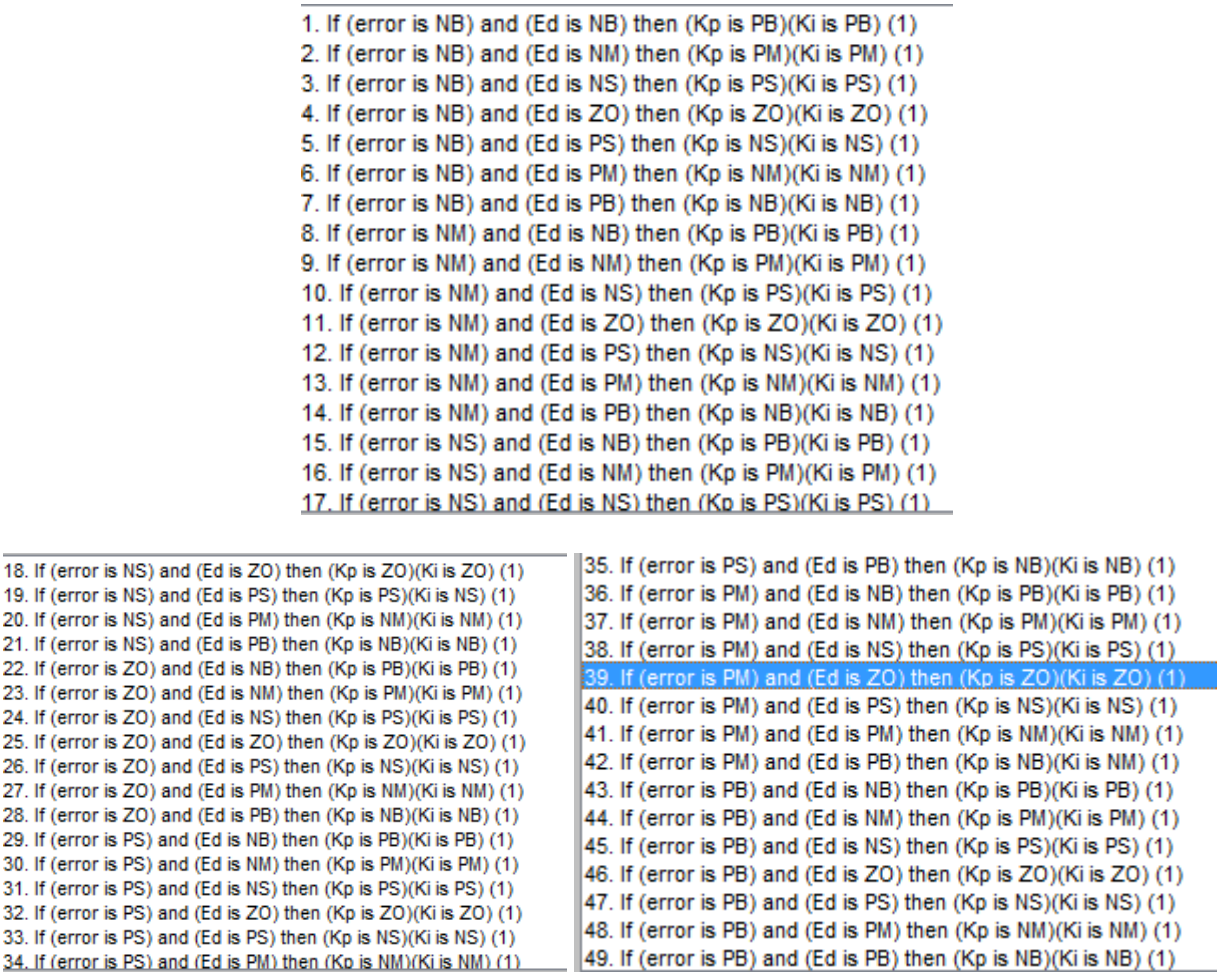

Fig 32c. Rules for V_DC Regulator

For modeling of current control circuitry, close loop secondary current of the transformer is used as reference current which will be not exceeded to 2000 amperes. An error is generated for using the secondary using reference 2000 amperes. This error is again comparing with the battery charging current and control the charging current of the battery using a Fuzzy Logic controller at a specific rating according to load demand. When the load is increased then charging current will decrease using this current control closed loop. When the load is decreased then charging current of the battery will be increased using this current control closed loop using Fuzzy Logic controller. Simulation diagram for current control loop (closed) and charging station controller are given in Figure-33(a, b and c).

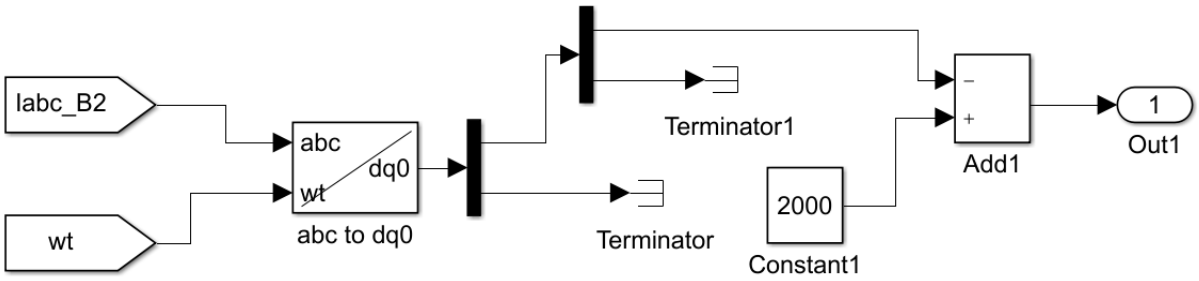

Fig 33a. Simulation Diagram for Current Control Closed Loop

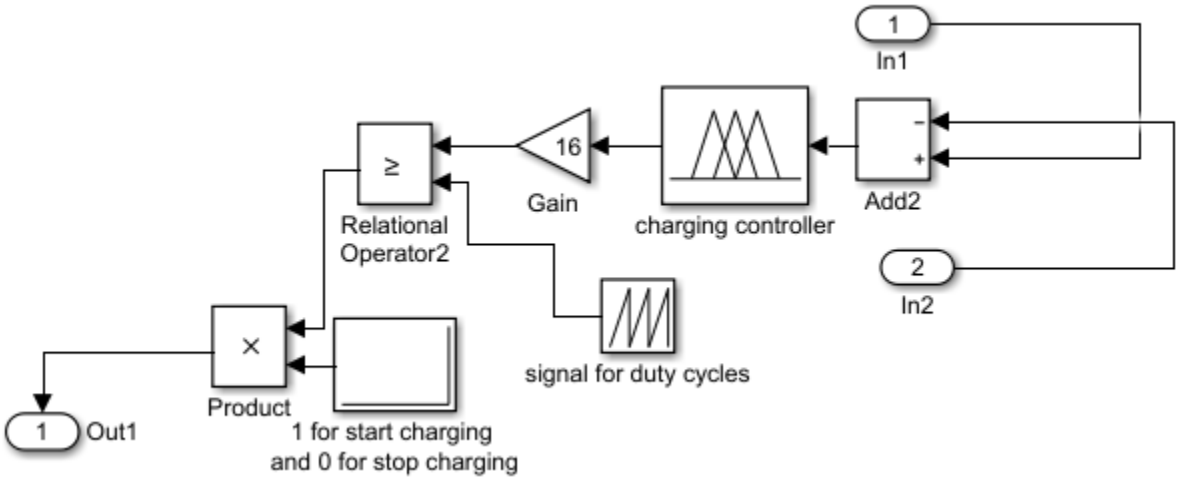

Fig 33b. Simulation Diagram for Charging Station Controller using Fuzzy Logic controller

Above diagram represents the fuzzy part of charging station control. To control the charging current of EV battery following membership functions is used for input and output:

Negative big (NB), Negative medium (NM), Negative small (NS), Zero (ZO), Positive small (PS), Positive medium (PM), Positive big (PB).

Following are the fuzzy rules for the charging station controller.

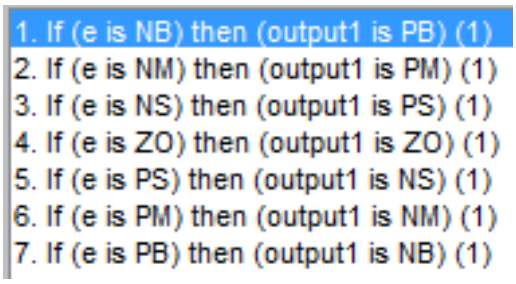

Fig 33c. Rules of Fuzzy Logic Charging Station Controller.

In the abnormal condition when power will transfer from the electric vehicle battery to grid, VSC pick reference parameters from slack bus B-1 but in this case, Idref is negative and bi-directional converter work as an inverter and inverts 500V DC into 240V AC. In this situation, dis-charging station controller discharges the battery according to load demand and power will deliver from V2G. In this case, discharging controller maintain 500 DC voltages at the DC load line by using two control loops, the external loop is voltage control loop and the internal control loop is the current control loop by using two Fuzzy Logic Controllers. Discharging station controller provides control duty cycle signal to MOSFET, for maintaining 500 DC voltages at DC lad line. Figure-34 (a, b and c) shows the discharging station controller.

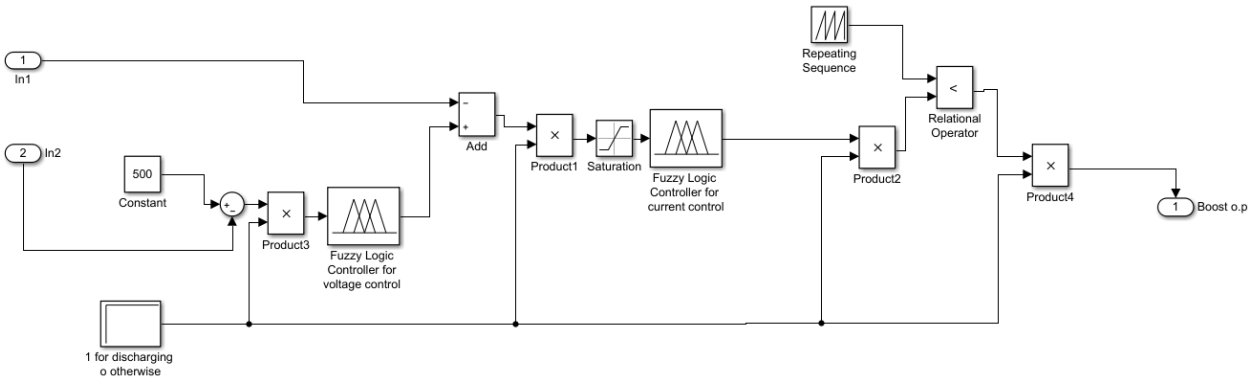

Fig 34a. Discharging Station Controller

The above diagram represents the Fuzzy part of the discharging station control. To control the discharging voltages and discharging current of the electric vehicle battery following membership functions are used for input and output:

NB (negative big), NM (negative medium), NS (negative small), ZO (zero), PS (positive small), PM (positive medium), PB (positive big).

Following are the fuzzy rules for discharging station voltage controller.

1. If (V_in is NB) then (V_out is PB) (1)
2. If (V_in is NM) then (V_out is PM) (1)
3. If (V_in is ZO) then (V_out is ZO) (1)
4. If (V_in is PS) then (V_out is NS) (1)
5. If (V_in is PM) then (V_out is NM) (1)
6. If (V_in is PB) then (V_out is NB) (1)
7. If (V_in is NS) then (V_out is PS) (1)

Fig 34b. Rules of Discharging Station Fuzzy Logic Voltages Controller

Following are the fuzzy rules for discharging station current controller.

1. If (I_in is NB) then (I_out is PB) (1)
2. If (I_in is NM) then (I_out is PM) (1)
3. If (I_in is NS) then (I_out is PS) (1)
4. If (I_in is ZO) then (I_out is ZO) (1)
5. If (I_in is PS) then (I_out is NS) (1)
6. If (I_in is PM) then (I_out is NM) (1)
7. If (I_in is PB) then (I_out is NB) (1)

Fig 34c. Rules of Discharging Station Fuzzy Logic Current Controller

4.3 Complete Simulink Model Of Grid.

In Figure 35 complete simulation model of the grid with VSC has been shown.

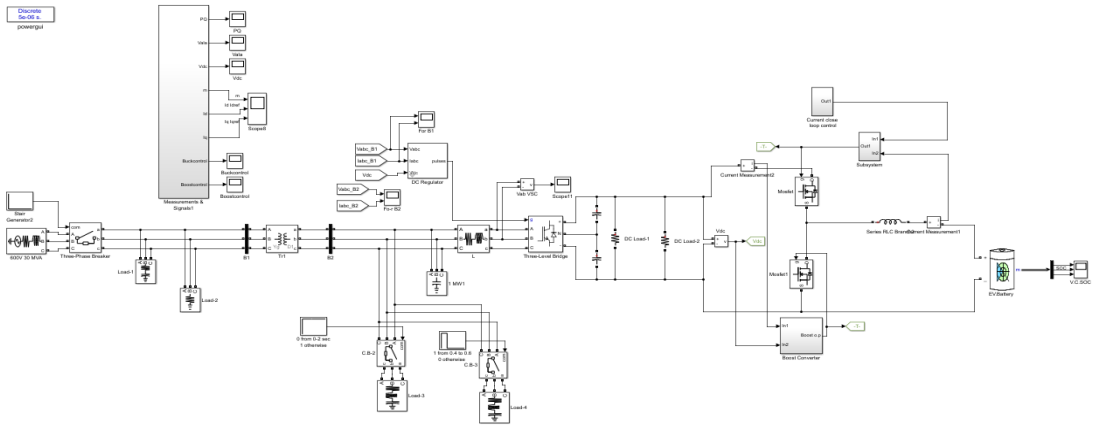

Fig 35. Simulink model of the Grid

4.4 Results & Discussion

Table.1 Parameters used in simulink model

Sr. No.	Component	Parameter/Rating
1	Transformer (11kV/400V)	104kVA
2	AC bus Voltage (line-line)	400V
3	VSC	100kVA
4	dc/dc converter	100kW
5	Dynamic load	36-126KW
6	Line resistance	2mΩ
7	Line reactance	2mH
8	Line capacitance	102.3μF
9	Battery storage at HV AC Bus	700V
10	dc side filter (765V)	4400μF
11	dc/dc converter inductance	6.2mH
12	dc/dc converter capacitance	450μF
13	VSC switching frequency	10kHz
14	dc/dc converter switching frequency	5kHz

A test case with simplified model of radial distributor is simulated. Total simulation time is set to be 0.3 sec. Figure 5 (a) and figure 5 (b) show load power with step changes and respective grid power fulfilling load demand, whereas Table 4 summarizes respective values. It can be seen that initial load is 36kW. 1st step change of 72kW in load occurs at 0.07 seconds and 2nd step change of 120kW in load occurs at 0.14 seconds. At 0.2 seconds islanding occurs and load is reduced to 40kW, however it goes to zero.

Figure 6 (a), (b) and (c) show load power, grid power and battery-storage power with overloading control. As evident in figure 6 (b) that during step changes and islanding mode, proposed overloading control with fuzzy control performs better than PI control in terms of overshoot, undershoot, rise time, settling time, steady state error and time to steady state. Similarly figure 6 (c) shows battery-storage's power to control the overloading during step changes and islanding. It is obvious that in this case fuzzy-control outperforms PI-control as

well. Figure 7 shows dc voltage at HV dc bus and it is again clear that fuzzy-control gives a better and stiffer voltage than PI-control. Figure 8 shows phase A of AC voltage and Current at LV AC bus. Again fuzzy-control gives a less deviated and less overshot voltage than PI-control. Tables 5 to 10 show this comparison in numeric values. Table 11 shows total harmonic distortion (THD) of v_{abc} at LV AC bus during both grid connected and islanded modes with both PI control and fuzzy control. As evident fuzzy-control has less THD as compared to PI-control.

Table 2

Power (kW)	**Constant load (kW)**	**1st step change in load (kW)**	**2nd step change in load (kW)**	**Islanding (kW)**
P_{load}	36	72	120	40
P_{grid}	104	104	104	0
$P_{battery\text{-}storage}$	68	32	-16	-40

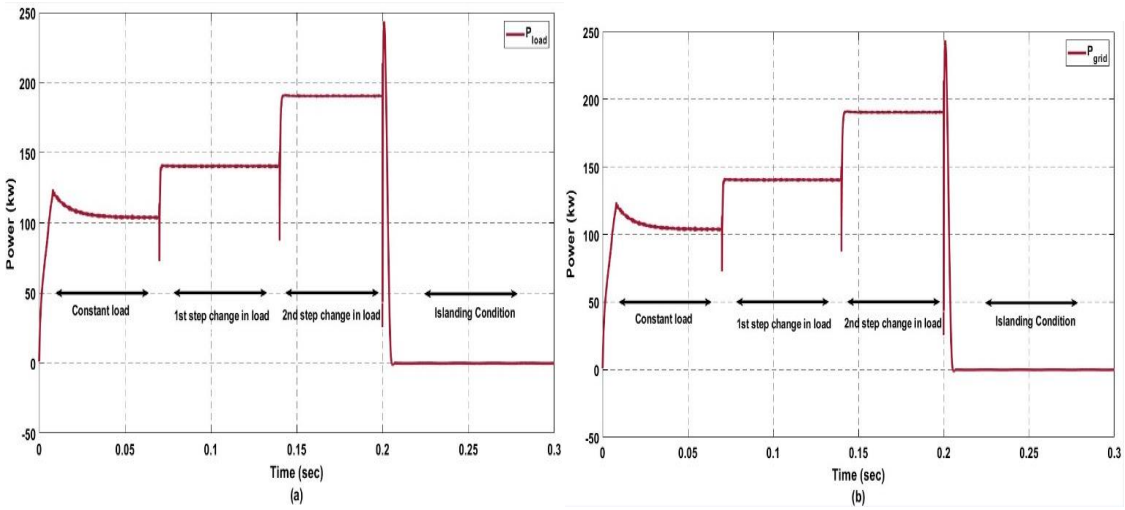

Fig 35. The complete simulation model of the system

Table 3

Indicator	**Constant load (sec)**	**1st step change in load (sec)**	**2nd step change in load (sec)**	**Islanding (sec)**
Overshoot	0	0	0	0
Undershoot	0	0.0715	0.15	0.206
Rise time	0.006	0.071	0.147	0.202
Settling time	0.0015	0.072	0.152	0.212
Steady state error	0	0.6%	3.3%	0
Time to steady state	0.0016	0.073	0.153	0.23

Table 3

Indicator	**Constant load (kW)**	**1st step change in load (kW)**	**2nd step change in load (kW)**	**Islanding (kW)**
Overshoot	0	0	0	0.204
Undershoot	0	0.0705	0.142	0
Rise time	0.006	0.0702	0.141	0.201
Settling time	0.0015	0.0715	0.145	0.21
Steady state error	0	0.4%	1%	0
Time to steady state	0.0015	0.0715	0.145	0.22

Table 4

Indicator	**Constant load (kW)**	**1st step change in load (kW)**	**2nd step change in load (kW)**	**Islanding (kW)**
Overshoot	0.0045	0.0707	0.141	0.201
Undershoot	0	0	0	0.202
Rise time	0.004	0.0704	0.1405	0.2006
Settling time	0.02	0.074	0.144	0.204
Steady state error	0	0	0	0
Time to steady state	0.04	0.075	0.155	0.2045

Table 5

Indicator	**Constant load (kW)**	**1st step change in load (kW)**	**2nd step change in load (kW)**	**Islanding (kW)**
Overshoot	0.004	0.0704	0	0.2005
Undershoot	0	0	0.1405	0
Rise time	0.003	0.0702	0.1402	0.2002
Settling time	0.01	0.0703	0.141	0.203
Steady state error	0	0	0	0
Time to steady state	0.02	0.072	0.152	0.204

Table 6

Indicator	**Constant load (kW)**	**1st step change in load (kW)**	**2nd step change in load (kW)**	**Islanding (kW)**
Overshoot	0.005	0	0	0.208
Undershhot	0	0.0703	0.145	0.214
Rise time	0.0045	0.0701	0.144	0.206
Settling time	0.022	0.0735	0.151	0.218
Steady state error	0	0	0	0
Time to steady state	0.03	0.076	0.153	0.224

Table 7

Indicator	**Constant load (kW)**	**1st step change in load (kW)**	**2nd step change in load (kW)**	**Islanding (kW)**
Over-shoot	0.004	0	0	0
Under-shoot	0	0.0701	0.143	0.21
Rise time	0.004	0.07	0.141	0.208
Settling time	0.01	0.0715	0.15	0.212
Steady state error	0	0	0	0
Time to steady state	0.015	0.073	0.151	0.215

Table 8

v_{abc} **@ LV AC bus**	**THD**
Grid-connected mode (fuzzy-control)	0.9%

Grid-connected mode (PI-control)	2.22%
Islanding mode (fuzzy-control)	0.78%
Islanding mode (PI-control)	1.24%

4.4.1 Results of PI controller-based Model

In this research use MATLAB 2017-A using discrete power GUI for simulation of the model. From 0 second to 0.8-second system is running in its normal mode and power will transfer from G2V and universal bridge work as a rectifier by using VSC, in this case, VSC pick reference point from slack bus B1 and Idref are positive and Id is negative then power will deliver from G2V. Two AC Loads, Load 1 and load 2 and two DC loads, Load-5 and Load-6 are connected continuously from 0sec to 1.2sec.

At 0.8sec to 1.2sec the grid switch to islanding mode and power will deliver from V2G and bidirectional universal bridge work as an inverter and inverts 500V DC to 240V AC by using VSC. In this case, VSC gets its reference values from slack bus B-1 but Idref is negative then power will deliver from V2G.

From Zero sec to 0.2sec only Electric vehicle battery will be connected to the grid through the charging station controller and charge at its full rating capacity.

At 0.2sec to 0.4sec load-3 will connect to grid so charging station controller control the charging of the battery and reduce charging current and protect the transformer to overloading.

From 0.4sec to 0.6sec Load 3 and load 4 both will be connected to grid so charging station controller control the charging of the battery to zero amperes and start discharging of the battery and provide active power to grid and protect the transformer to overloading.

From 0.6sec to 0.8sec load 4 will disconnect from the grid so charging station controller again charge the battery to its desired rating.

From 0.8sec to 1.2sec grid switch to islanding mode and power will deliver from the battery to the grid through discharging controller and state of charge of the battery will be reduced and provide the power to load 1, Load 2, and Load 3.

In Figure 36 Vabc B1, Iabc B1 and in Figure 37 VabcB2 and Iabc B2 are shown.

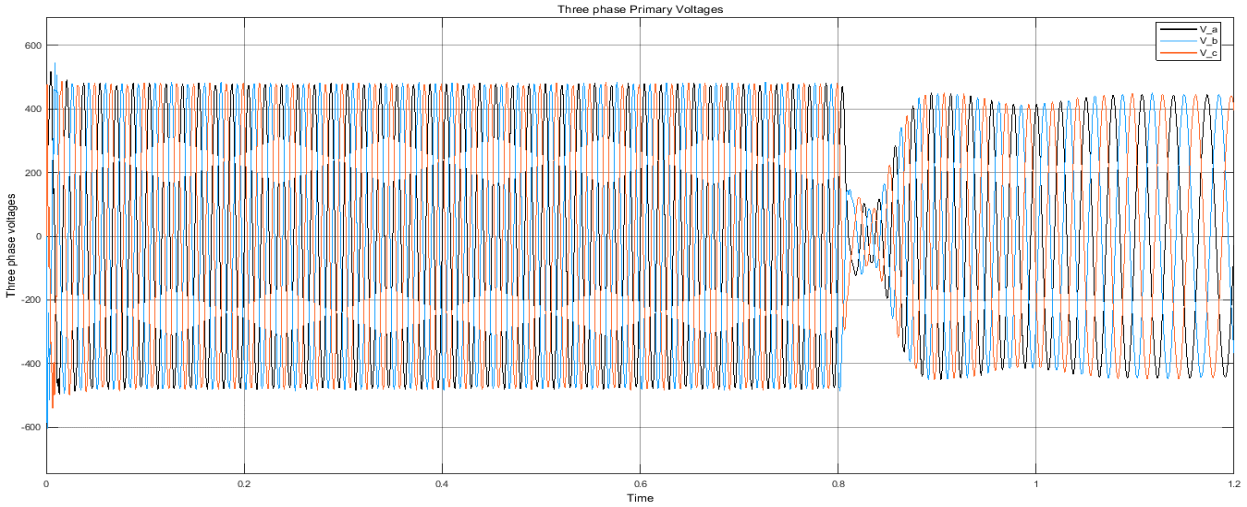

Fig 36a. Vabc-B1

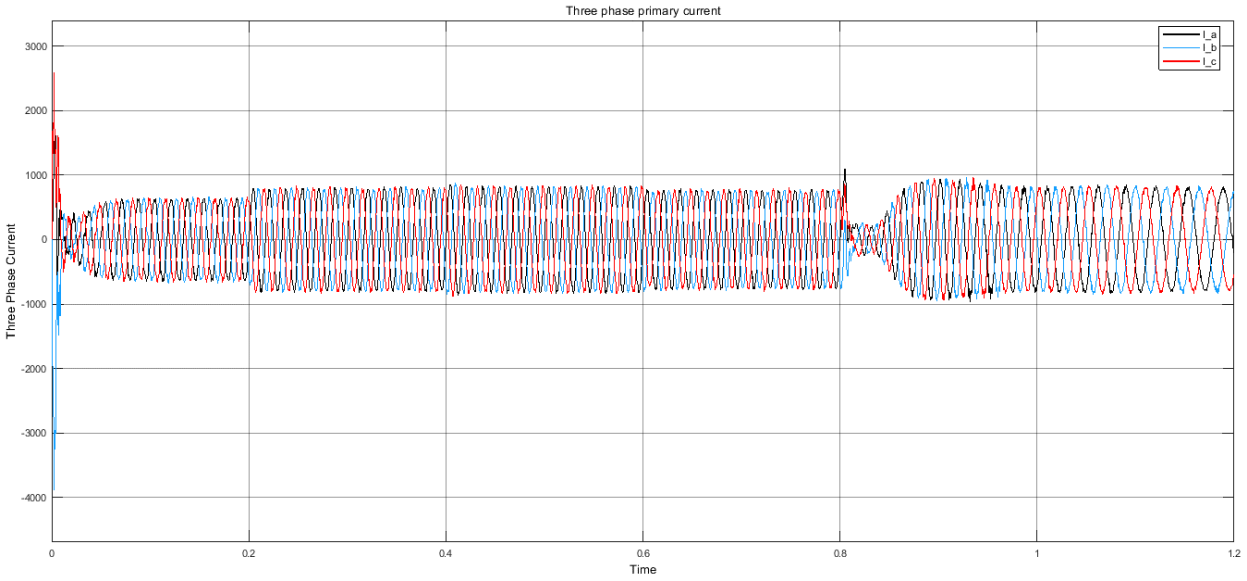

Fig 36b. Iabc-B1

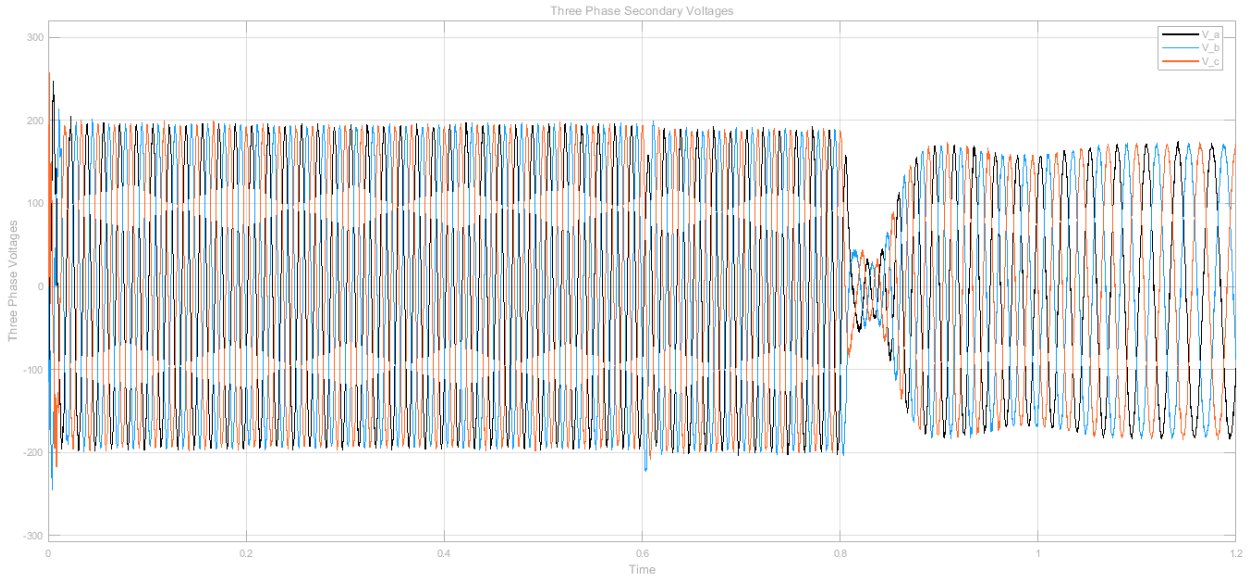

Fig 37a. Vabc-B2

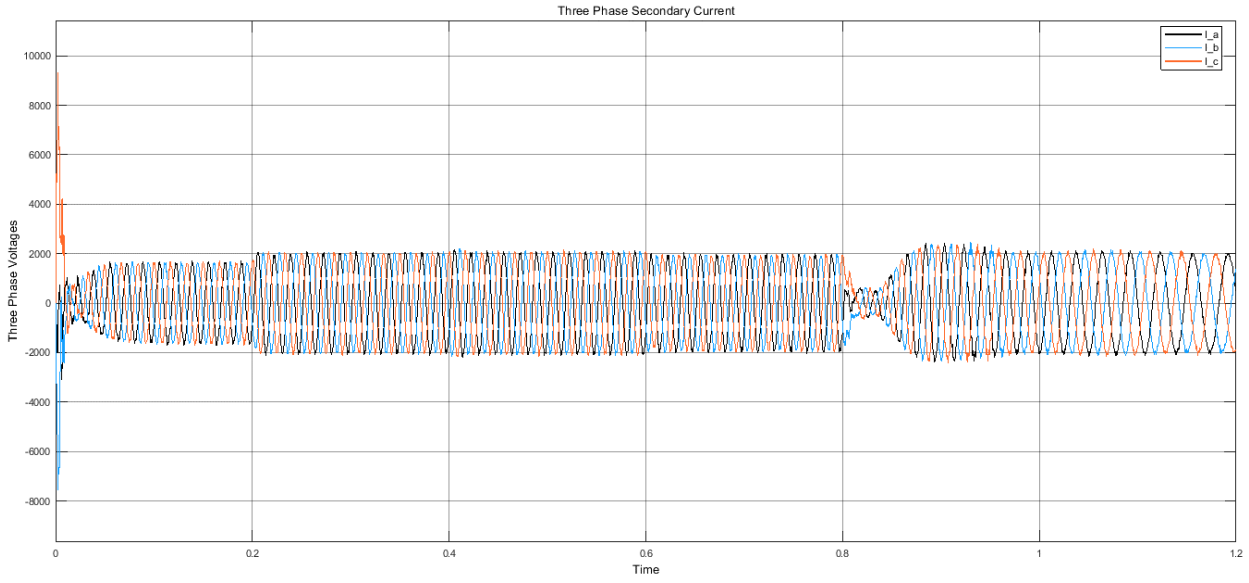

Fig 37b. Iabc-B2

In Figure 38 DC load line 500 DC voltages are shown and in Figure 39 show the Vabc of the three-phase 240 AC voltages at the transformer secondary side.

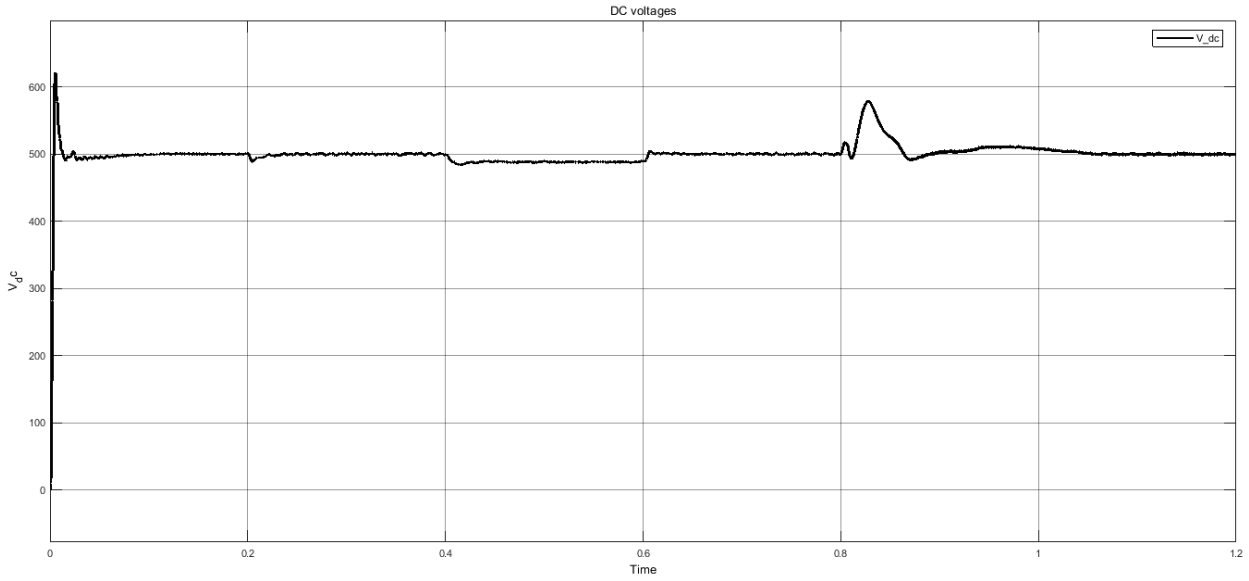

Fig 38. Vdc

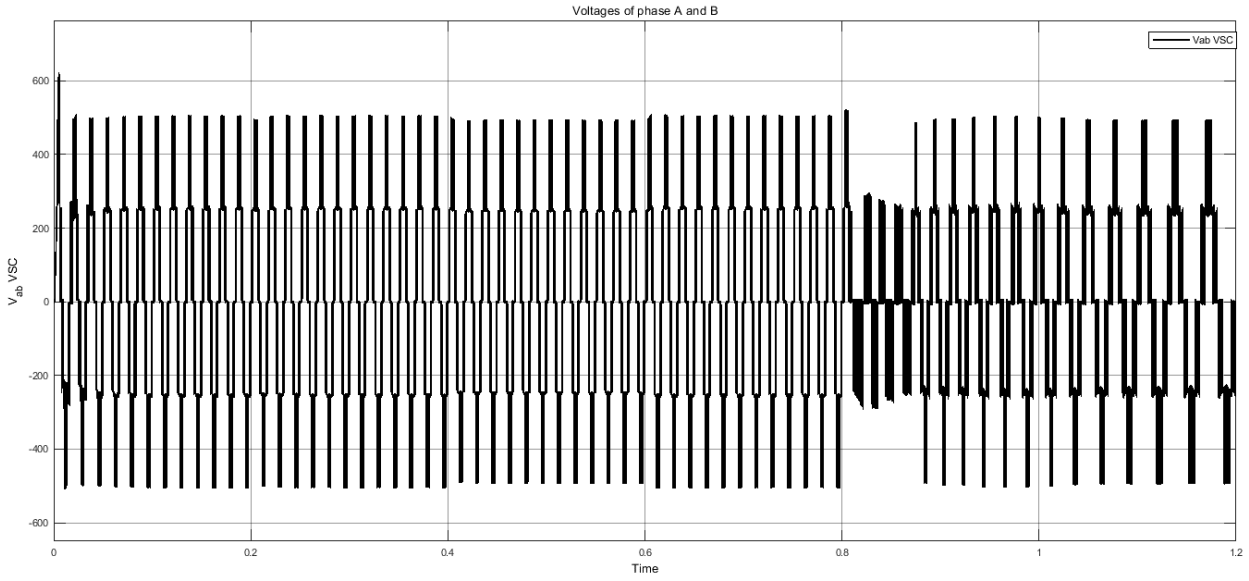

Fig 39. Vab-Vsc

Power will deliver from G2V during normal operation and as a result voltages and current are in phase to each other.

In abnormal operation, when power will deliver from battery to grid then voltage and current are out of phase by 180 degrees to each other. Va and Ia are shown in Figure 40.

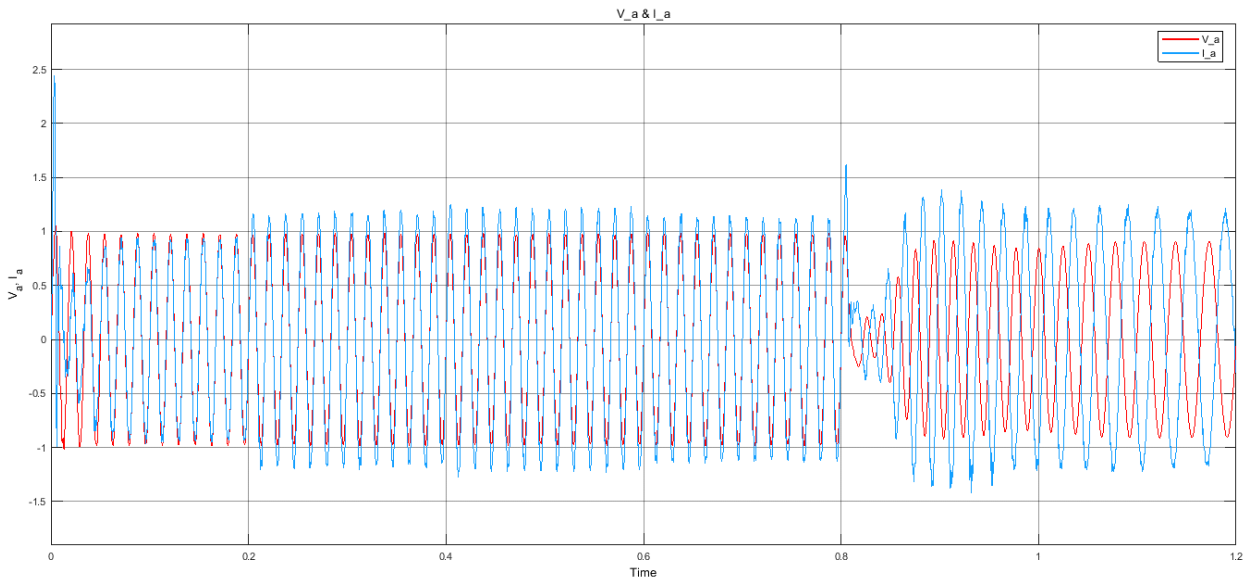

Fig 40. VaIa

In Figure 41 battery, current is shown. From 0sec to 0.2sec battery charge at its full rating, from0.2 to 0.4sec battery current will reduce, from 0.4sec to 0.6sec battery will discharge, from 0.6sec to 0.8-sec battery again charge at its normal rating. From 0.8 sec to 1.2-sec battery will be discharged according to load demand.

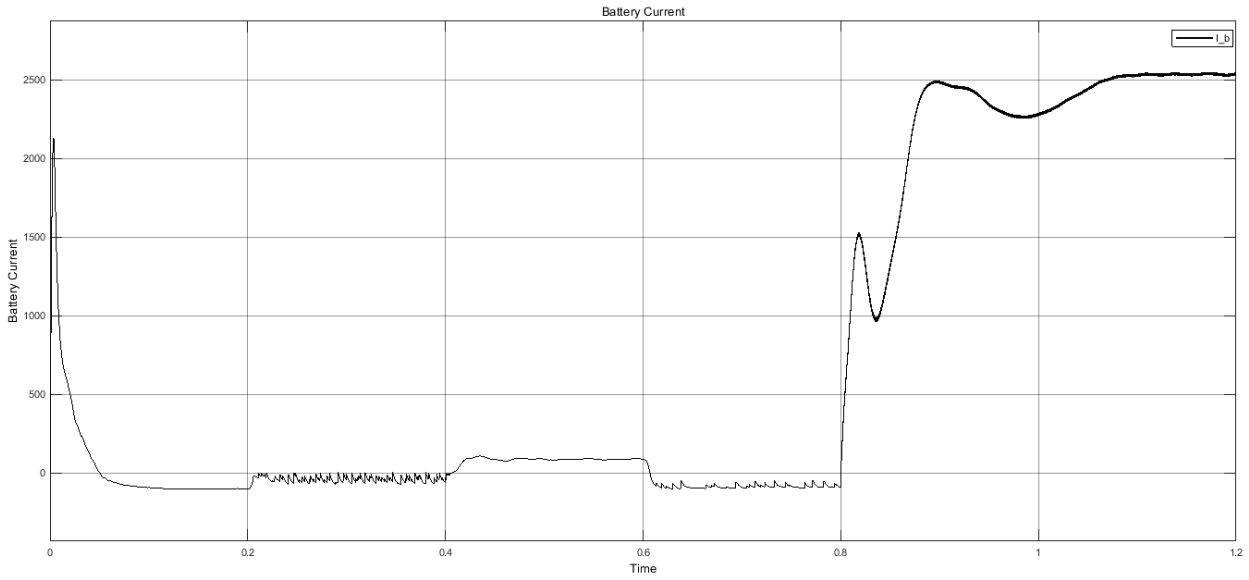

Fig 41. Battery Current

In Figure-42 show the (id and idref), (iq and iqref) and modulation index of the VSC.

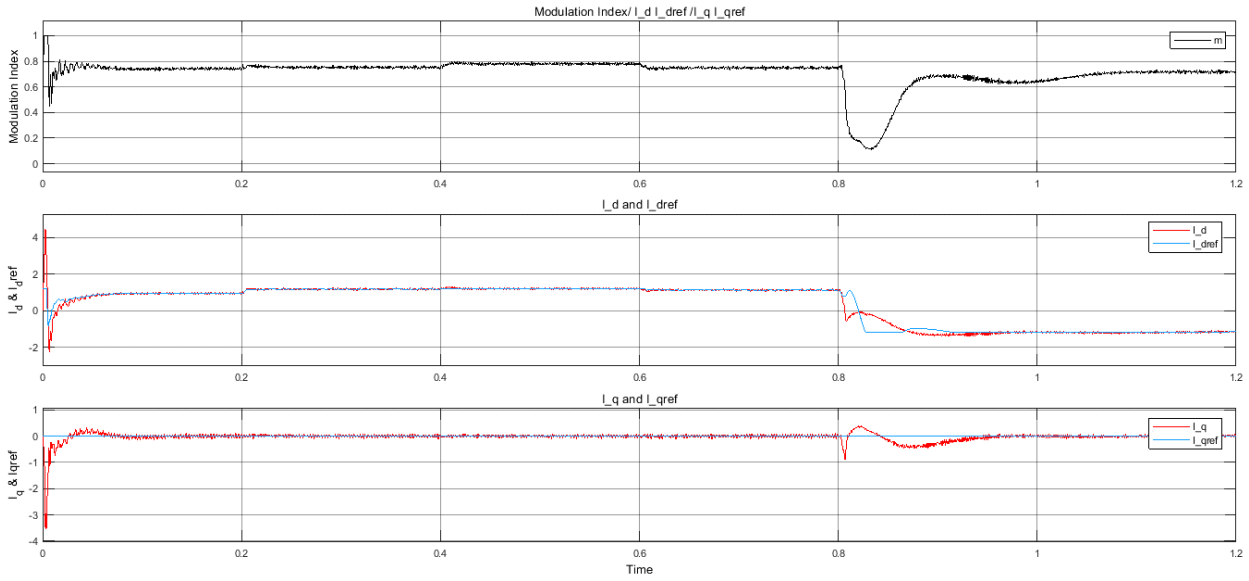

Fig 42. (I_D, I_Dref), (I_Q, I_Qref), and VSC Modulation Index

Figure 43 and 44 shows the controlling pulses of charging station controller and discharging station controller.

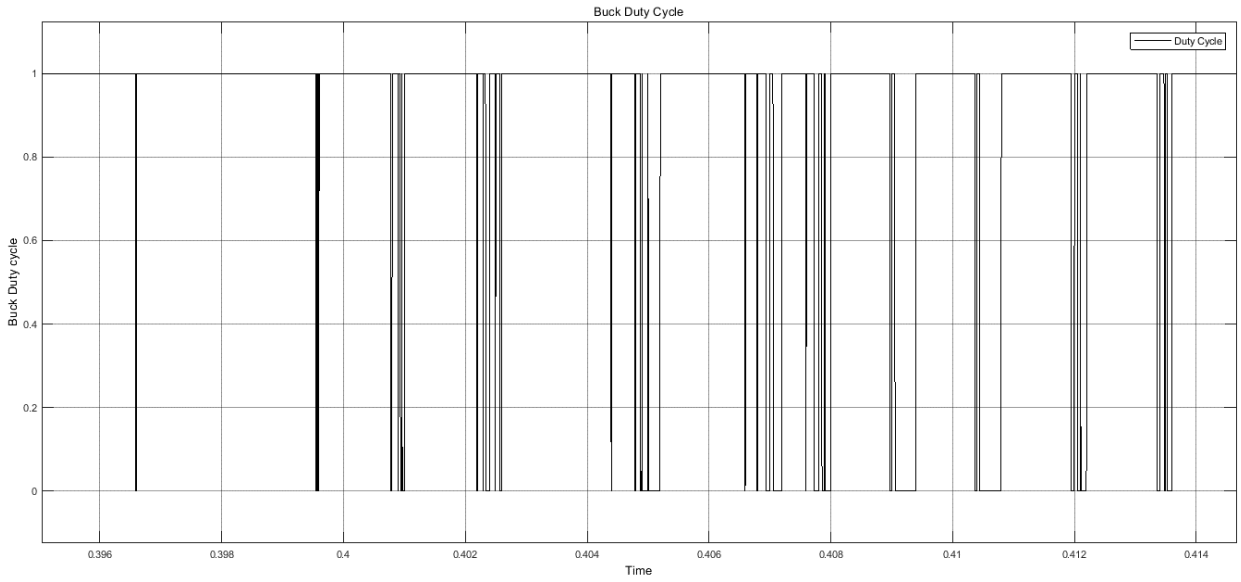

Fig 43. Charging Station Controller Pulses

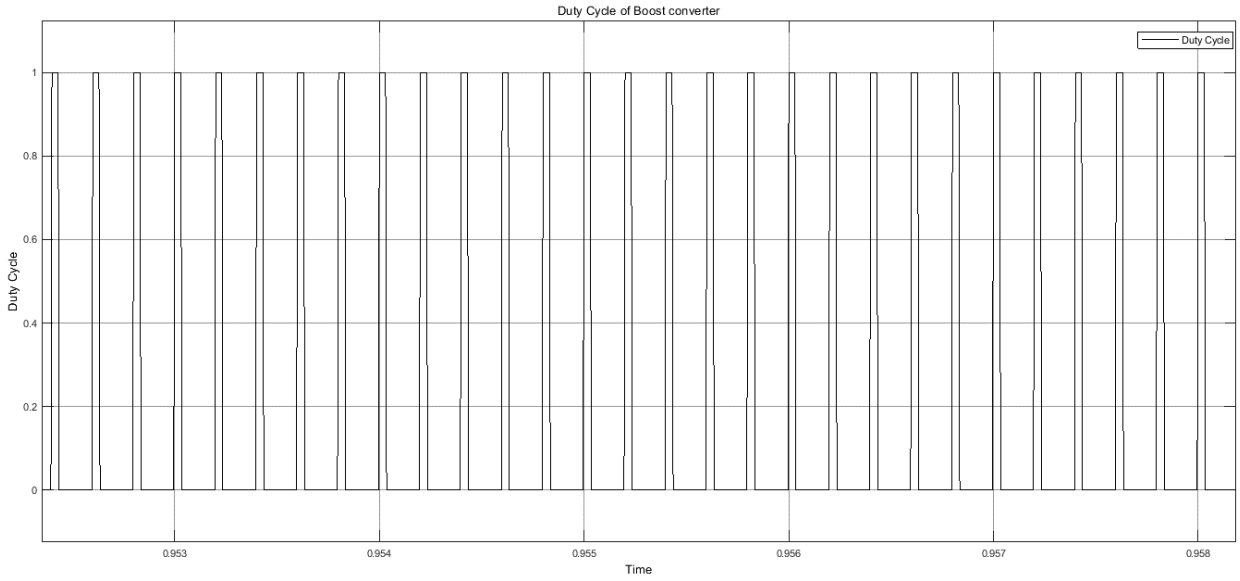

Fig 44. Discharging Station Controller Pulses

4.4.2 The result of a Fuzzy Controller based Model

In Figure 45 Vabc B1and Iabc B1 are shown. In Figure 46 Vabc B2, Iabc B2 are shown. In Figure-47 VDC are shown. In Figure 48 Vab VSC is shown. In Figure 49 VaIa is shown. In Figure 50 Battery SOC, battery current and battery voltages are shown. In Figure 51 Id Idref, Iq Iqref and Modulation index of VSC are shown. In Figure 52 control pulses of the charging station controller are shown. In Figure 53 control pulses of discharging station controller are shown.

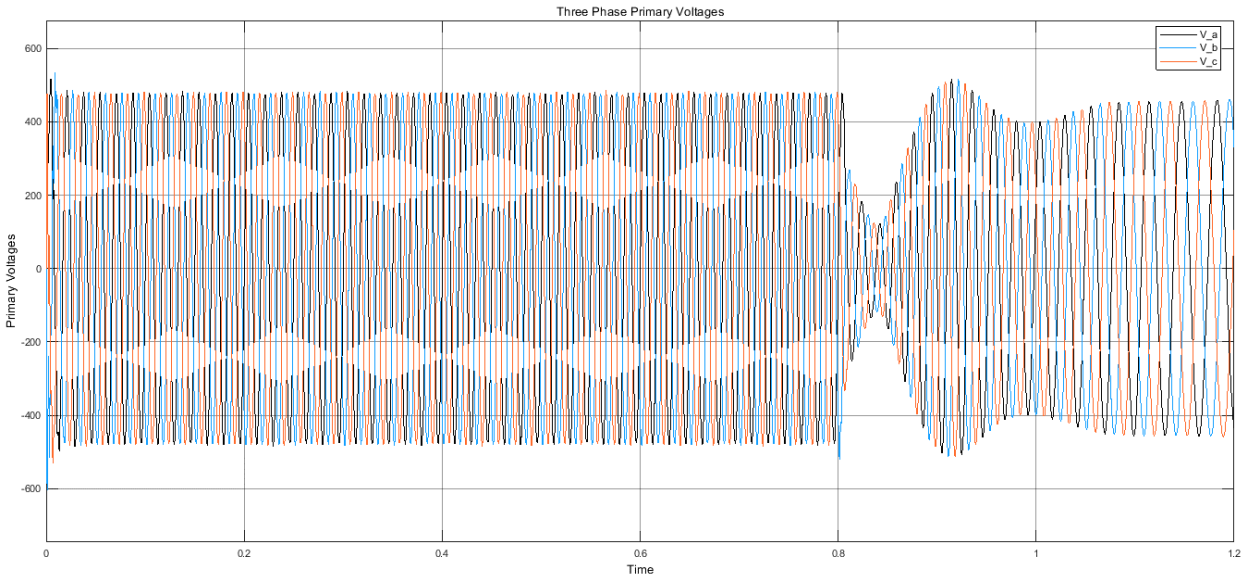

Fig 45a. Vabc B1

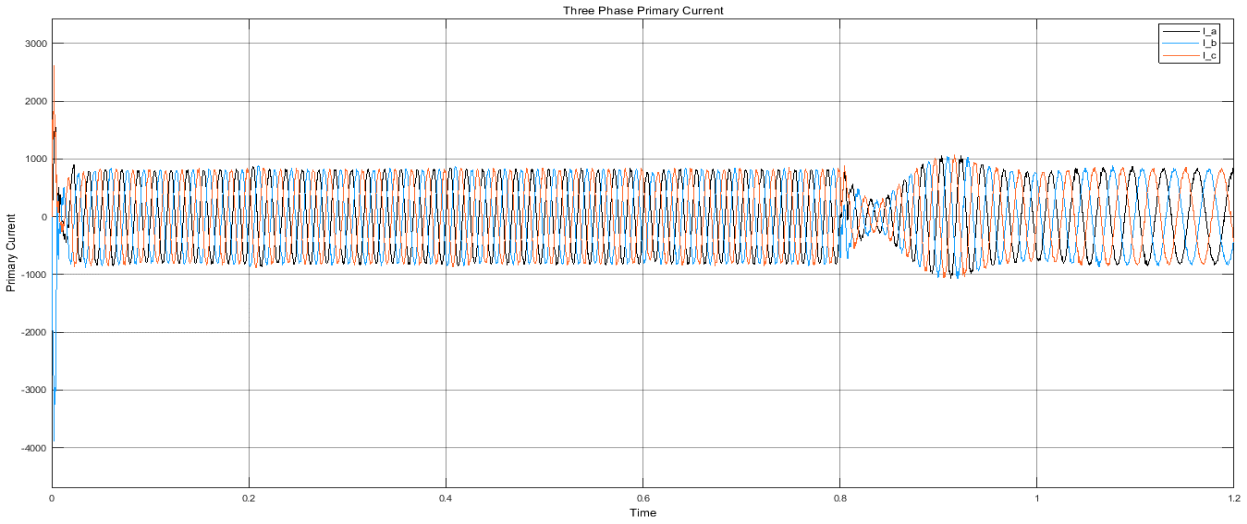

Fig 45b. Iabc B1

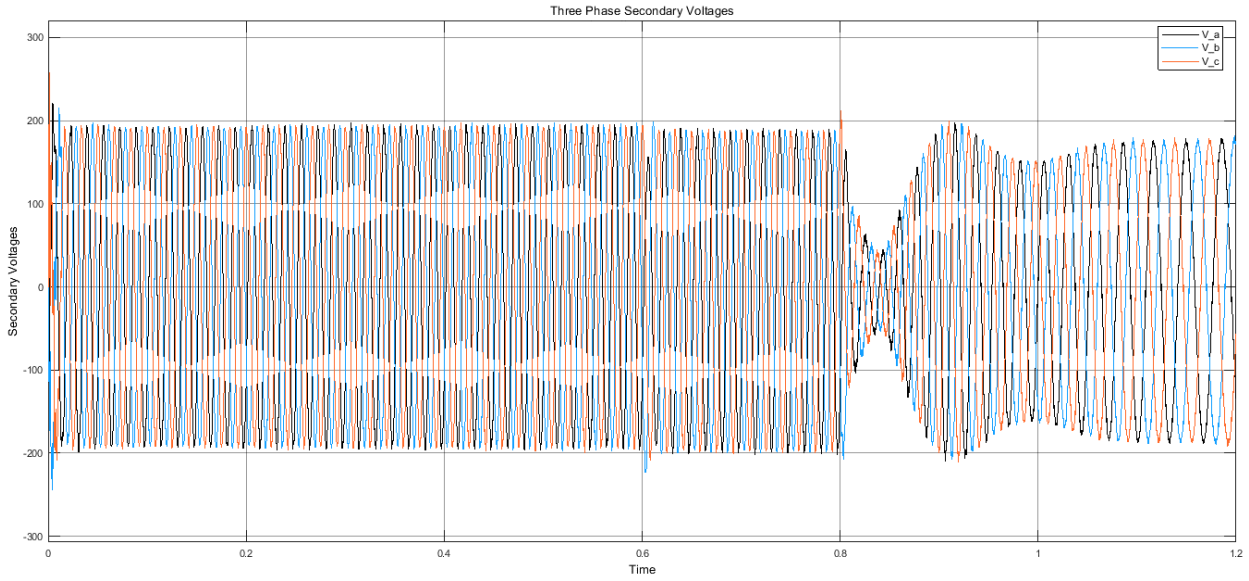

Fig 46a. Vabc B2

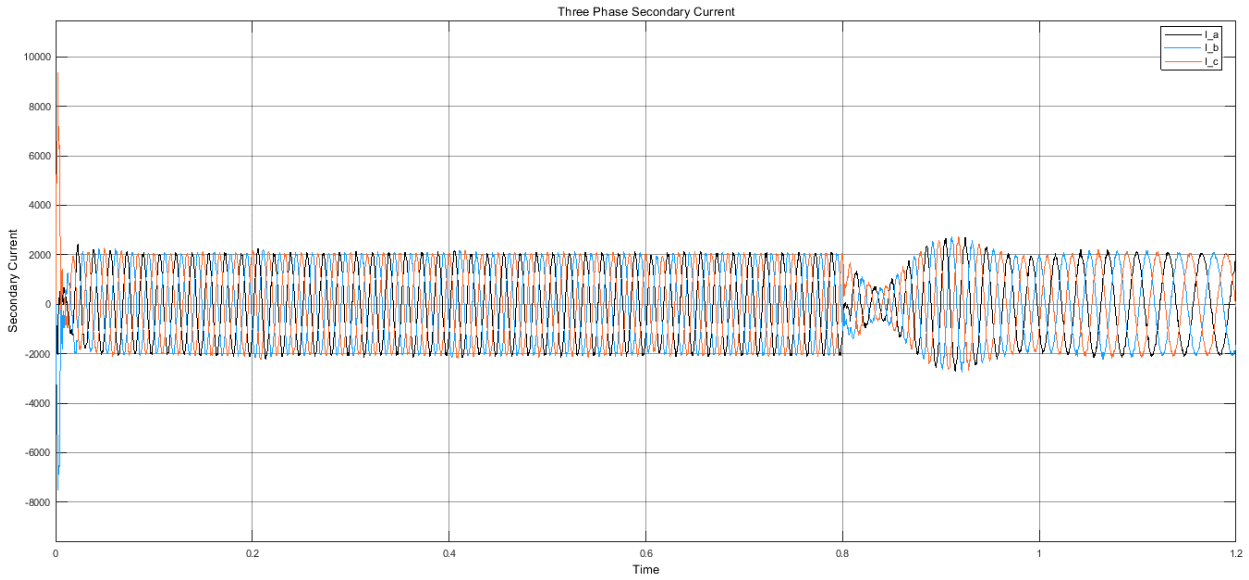

Fig 46b. Iabc B2

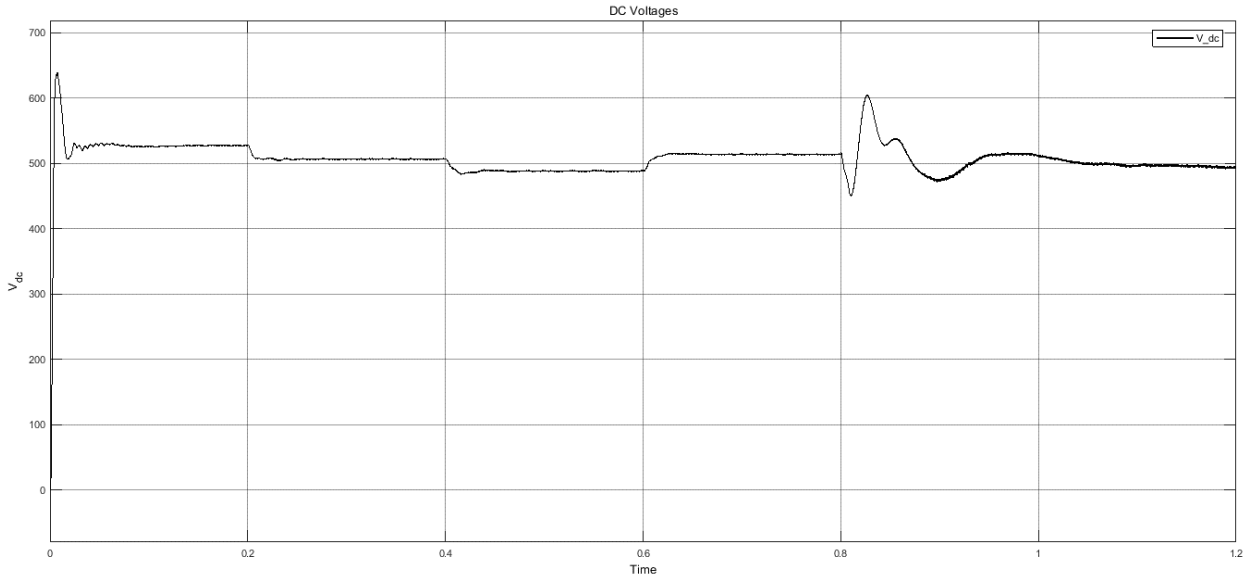

Fig 47. VDC

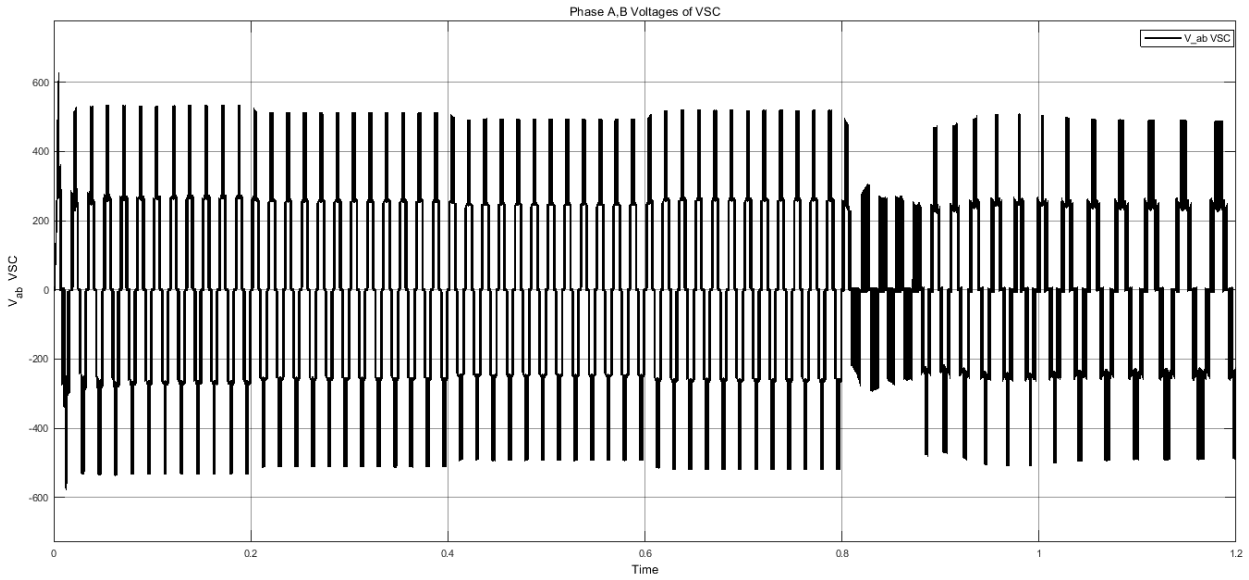

Fig 48. Vab VSC

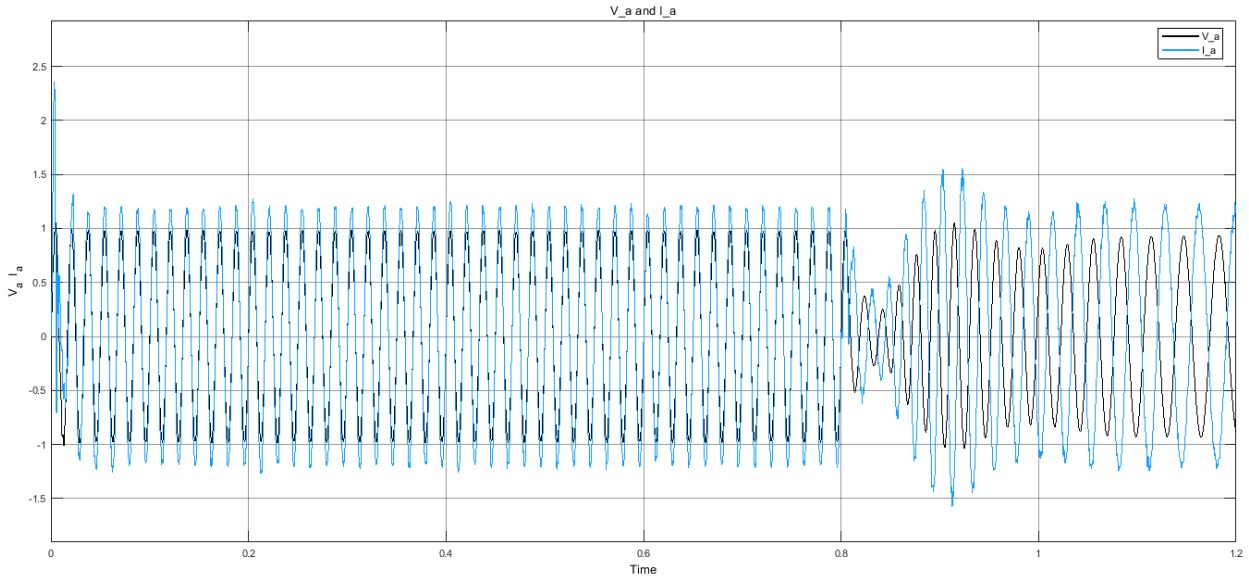

Fig 49. Va_Ia

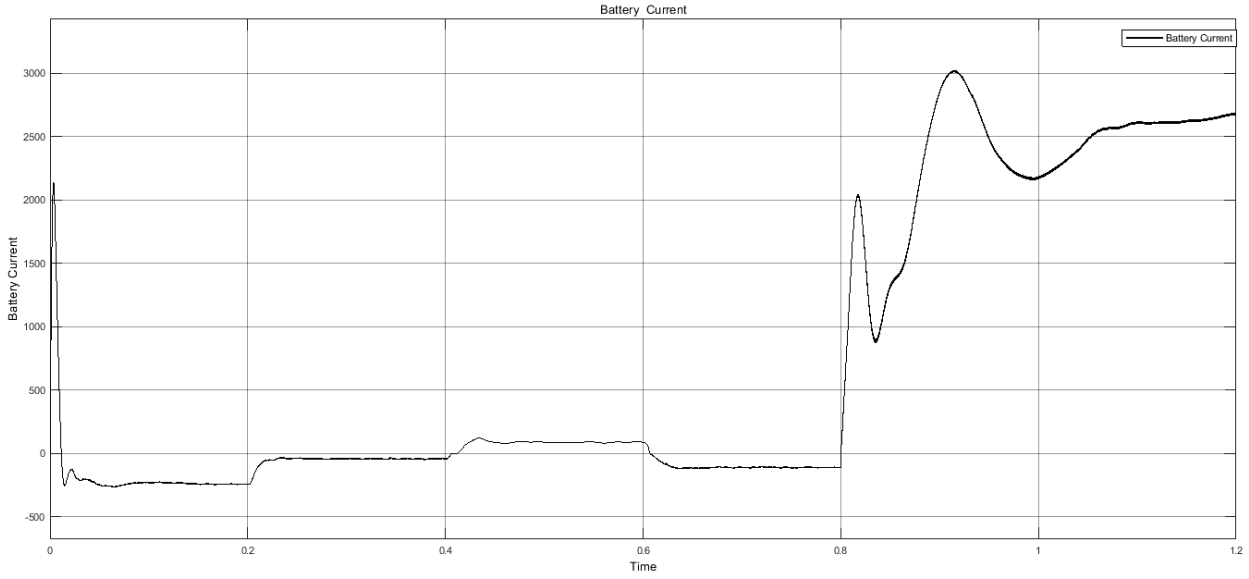

Fig 50a. Battery current

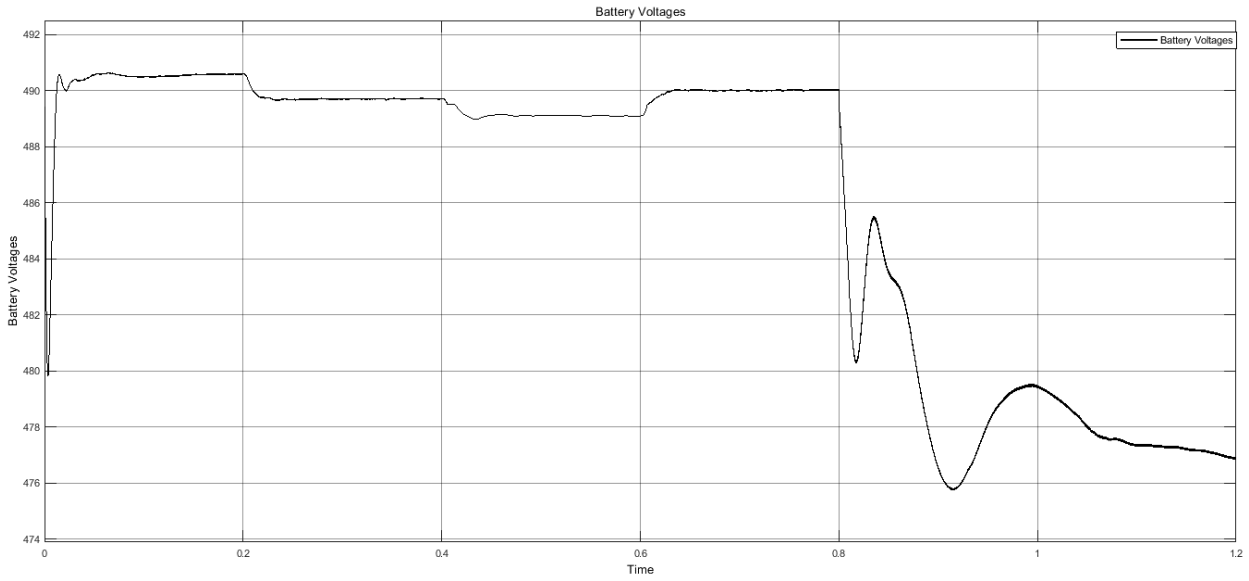

Fig 50b. Battery voltages

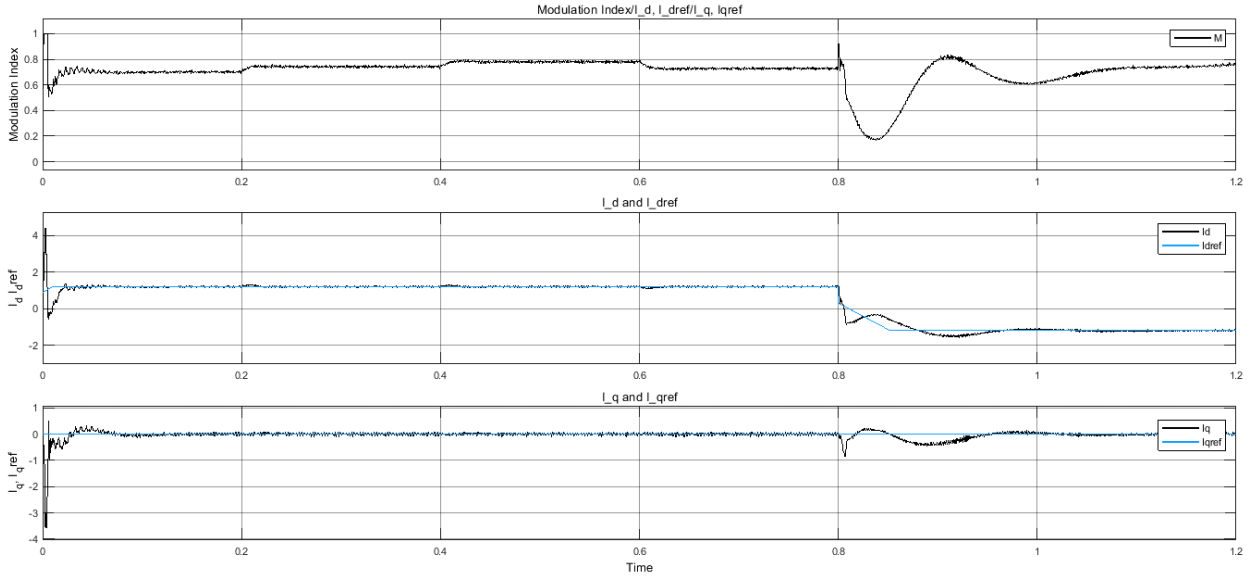

Fig 51. (I_d, I_dref), (Iq, Iq_ref) and Modulation index of VSC.

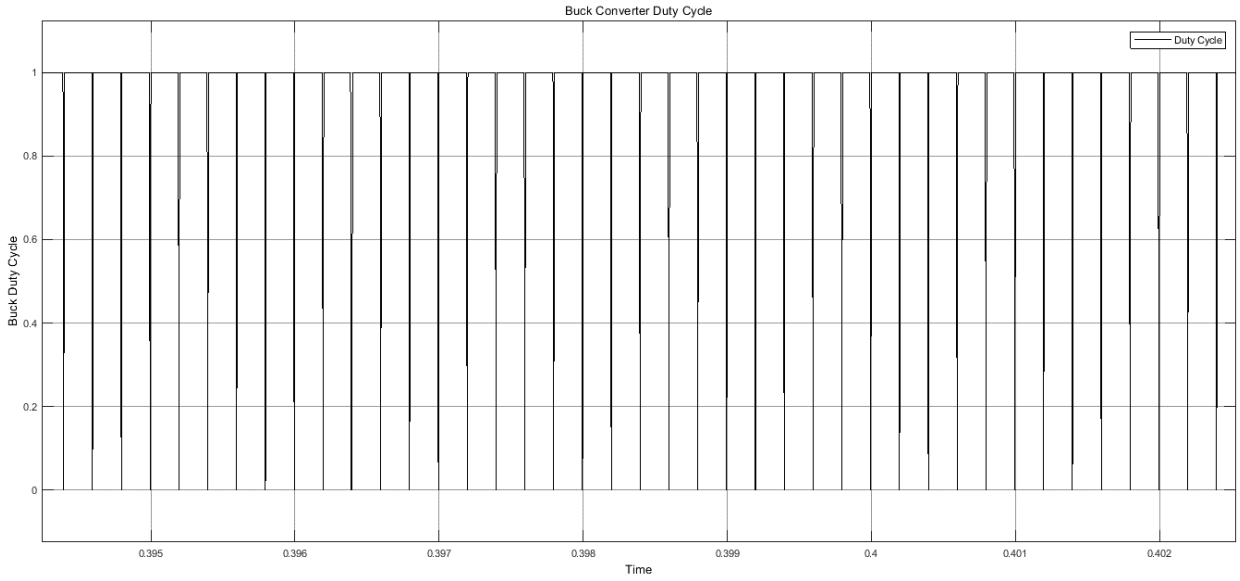

Fig 52. Control pulses of charging station.

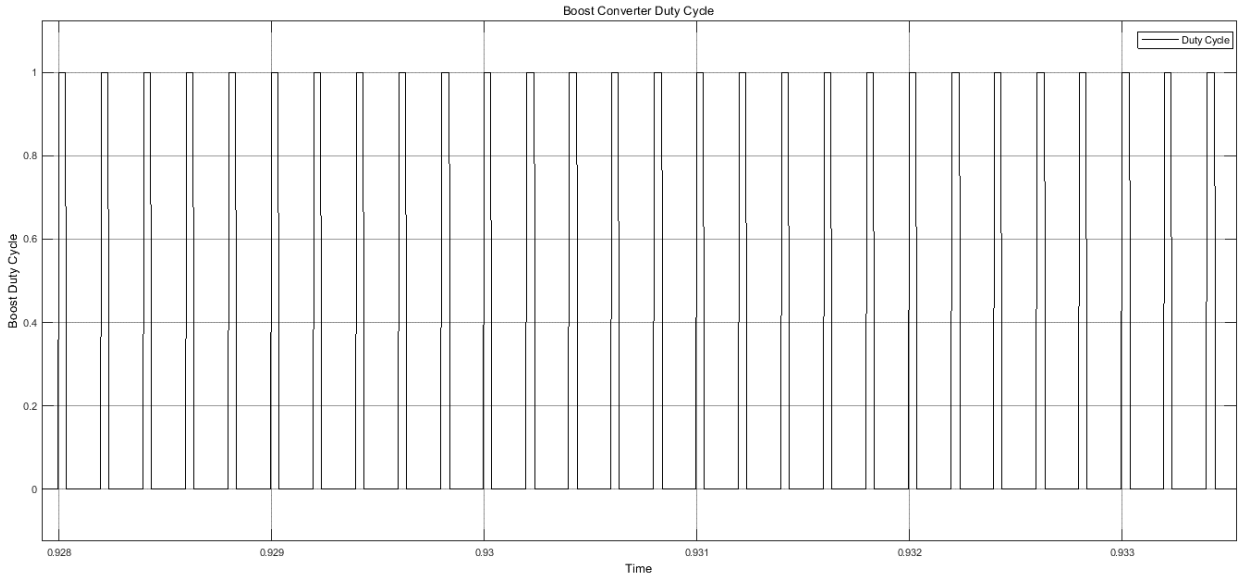

Fig 53. Control pulses of discharging station.

Chapter 5

Conclusion & Future work

CONCLUSION AND FUTURE WORK

From the test results, it can be concluded that when the load is less at the secondary side of the distribution transformer then the battery will charge at full rating capacity. When the load is increased then the charging of the battery will be decreased. When the load is increased from a specified limit then the battery will be discharged. When the utility grid is a switch to islanding mode then battery work as a distributed energy source and provides power to load. In this case, power will deliver from vehicle to grid.

By controlling the charging and discharging of the battery load side management will achieve without load shedding, in case of overloading of the distribution system. In case of islanding of the utility grid, battery provides power to the utility grid and enhances the transient stability of the grid in both load variation and islanding modes.

In the future, battery and D-STATCOM co-ordination will be performed using the droop control. Active power will be provided from the battery and reactive power will be provided from the STATCOM. In normal case when the load will be small then battery consume active power and STATCOM consume reactive power as per their requirement. In overloading condition, battery charging will be controlled and battery consumes less active power and D-STATCOM will consume less reactive power. After a specific value of overloading battery will discharge to the grid and provide the active power to load and D-STATCOM provide the reactive power to load by using droop control. In the case of islanding, the battery provides active power to grid and D-STATCOM provide reactive power to the grid by using droop control.

With the help of battery and D-STATCOM coordination load side management and transient stability will be achieved without load shedding in both load variation and islanding modes.

REFERENCES

[1] Rajashree Dhua, Debashis Chatterjee, and Swapan Kumar Goswami. Study of Improved Load Sharing Methodologies for Distributed Generation Units Connected in a Microgrid, CSEE JOURNAL OF POWER AND ENERGY SYSTEMS, VOL. 3, NO. 3, September 2017.

[2] Xiaokang Xu, Martin Bishop, Donna G. Oikarinen, and Chen Hao, Application and Modeling of Battery Energy Storage in Power Systems, CSEE JOURNAL OF POWER AND ENERGY SYSTEMS, VOL. 2, NO. 3, September 2016.

[3] Joan Rocabert, Alvaro Luna, Frede Blaabjerg, and Pedro Rodr´ıguez, Control of Power Converters in AC Microgrids IEEE TRANSACTIONS ON POWER ELECTRONICS, VOL. 27, NO. 11, November 2012.

[4] Ritwik Majumder. Some Aspects of Stability in Microgrids, IEEE TRANSACTIONS ON POWER SYSTEMS, VOL. 28, NO. 3, August 2013.

[5] Mukesh Singh, Praveen Kumar, and Indrani Kar, Implementation of Vehicle to Grid Infrastructure Using Fuzzy Logic Controller, IEEE TRANSACTIONS ON SMART GRID, VOL. 3, NO. 1, MARCH 2012.

[6] Principles of Electrical Machines by V.K METHA and ROHIT METHA 5th Edition.

[7] An LC Filter Design Method for Single-phase PWM Inverters, IEEE catalog No.95TH 80250-7803-2423/95, by Pekik A.Dahono, Agus Purwari, and Qamaruzzaman, Institute Technology Bandung, J1 INDONESIA.

[8] Voltage source inverter Reference Design, by Texas Instruments Incorporated, TIDUAY6C-November 2015-Revised November 2017.

[9] The Discrete Model of the Power Stages of the Voltage Source Inverter For UPS, Zbigniew Rymarski, Article in International Journal of Electronics October 2011. Institute of Electronics, Silesian, University of Technology, Gliwice, Poland.

[10] Power electronics circuit devices and applications, Muhammad H.Rashid 3rd Edition, 2004

[11] The Discrete Evaluating noise and DC offset due to interharmonics and supra-harmonics caused by the back-to-back converter of (DFIG) in AC distribution network 24th International

Conference & Exhibition on Electricity Distribution (CIRED) 12-15 June 2017, Alireza Alizade, Javad Behkesh Noshahr

[12] Fault Ride-Through Capability Enhancement Strategy for VSC-HVDC Systems Supplying for Passive Industrial Installations, IEEE TRANSACTIONS ON POWER DELIVERY, VOL. 31, NO. 4, AUGUST 2016, Zhipeng Bian and Zheng Xu, Member, IEEE.

[13] Design considerations of superconducting fault current limiters for power system stability enhancement, IET Generation, Transmission & Distribution, on 23rd June 2017, Surour Alaraifi, Mohamed Shawky El Moursi.

[14] Optimal placement of static compensators for multi-objective voltage stability enhancement of power systems, IET Generation, Transmission & Distribution, on 24th June 2015, Yan Xu, Zhao Yang Dong, Chixin Xiao, Rui Zhang, Kit Po Wong.

[15] Reactive Power Compensation Capabilities of V2G-Enabled Electric Vehicles, IEEE TRANSACTIONS ON POWER ELECTRONICS, VOL. 32, NO. 12, DECEMBER 2017, Giuseppe Buja, Life Fellow, IEEE, Manuele Bertoluzzo, and Christian Fontana, Member, IEEE.

[16] Authentication Scheme for Flexible Charging and Discharging of Mobile Vehicles in the V2G Networks, IEEE TRANSACTIONS ON INFORMATION FORENSICS AND SECURITY, VOL. 11, NO. 7, JULY 2016, Neetesh Saxena, Member, IEEE, and Bong Jun Choi, Member, IEEE

[17] Optimal, Nonlinear, and Distributed Designs of Droop Controls for DC Microgrids, IEEE TRANSACTIONS ON SMART GRID, VOL. 5, NO. 5, SEPTEMBER 2014, Ali Maknouninejad, Member, IEEE, Zhihua Qu, Fellow, IEEE, Frank L. Lewis, Fellow, IEEE, and Ali Davoudi, Member, IEEE

[18] Distributed Secondary Voltage and Frequency Restoration Control of Droop-Controlled Inverter-Based Microgrids, IEEE TRANSACTIONS ON INDUSTRIAL ELECTRONICS, VOL. 62, NO. 7, JULY 2015. Fanghong Guo, Changyun Wen, Fellow, IEEE, Jianfeng Mao, Member, IEEE, and Yong-Duan Song, Senior Member, IEEE.

[19] Fully Distributed Hierarchical Control of Parallel Grid-Supporting Inverters in Islanded AC Microgrids, IEEE TRANSACTIONS ON INDUSTRIAL INFORMATICS, VOL. 14, NO. 2, FEBRUARY 2018 Zhongwen Li, Student Member, IEEE, Chuanzhi Zang, Peng Zeng, Haibin Yu, and Shuhui Li, Senior Member, IEEE

[20] Enhanced Power Flow Control for Grid-Connected Droop-Controlled Inverters With Improved Stability, IEEE TRANSACTIONS ON INDUSTRIAL ELECTRONICS, VOL. 64, NO. 7, JULY 2017. Yan Deng, Yong Tao, Guipeng Chen, Guangdi Li, and Xiangning He, Fellow, IEEE

[21] A New Design Method for the Passive Damped LCL and LLCL Filter-Based Single-Phase Grid-Tied Inverter, IEEE TRANSACTIONS ON INDUSTRIAL ELECTRONICS, VOL. 60, NO. 10, October 2013. by Weimin Wu, Yuanbin He, Tianhao Tang, Senior Member, IEEE, and Frede Blaabjerg, Fellow, IEEE

[22] LLCL-Filter Based Single-Phase Grid-Tied Aalborg Inverter, 978-1-4799-6768-1/14/$31.00 ©2014 IEEE Min Huang, Frede Blaabjerg Dept. of Energy Technology Aalborg University Aalborg, Demark.

[23] Effect of Asymmetric Layout of IGBT Modules on Reliability of Power Inverters in Motor Drive System, Ui-Min Choi, Ionut Veronica and Frede Blaabjerg Center of Reliable Power Electronics (CORPE) Department of Energy Technology, Aalborg University Aalborg, Denmark, 978-1-5386-1180-7/18/$31.00 ©2018 IEEE

[24] Modeling and Analysis of Harmonic Stability in an AC Power-Electronics-Based Power System, IEEE TRANSACTIONS ON POWER ELECTRONICS, VOL. 29, NO. 12, DECEMBER 2014 by Xiongfei Wang, Member, IEEE, Frede Blaabjerg, Fellow, IEEE.

[25] Unipolar Single Reference Multicarrier Sinusoidal Pulse Width Modulation Based 7-level Inverter with Reduced Number of Semiconductor Switches for Renewable Energy Applications, 978-1-5386-4198-9/18/$31.00 ©2018 IEEE, by Frede Blaabjerg Center of Reliable Power Electronics (CORPE), Dept. of Energy Technology, Aalborg University, Denmark. fbl@et.aau.dk

[26] A Transient Stability Assessment Framework in Power Electronic-Interfaced Distribution Systems. IEEE TRANSACTIONS ON POWER SYSTEMS, VOL. 31, NO. 6, November 2016. By Yun Zhang, Student Member, IEEE, and Le Xie, Member, IEEE.

[27] Transient Stability Augmentation of PV/DFIG/SG-Based Hybrid Power System by Nonlinear Control-Based Variable Resistive FCL, IEEE TRANSACTIONS ON SUSTAINABLE ENERGY, VOL. 6, NO. 4, October 2015, by Md. Kamal Hossain, Student Member, IEEE, and Mohd. Hasan Ali, Senior Member, IEEE.

[28] Surrogate Modeling-Based Multi-Objective Dynamic VAR Planning Considering Short-Term Voltage Stability and Transient Stability, IEEE TRANSACTIONS ON POWER SYSTEMS,

VOL. 33, NO. 1, JANUARY 2018, by Tong Han, Student Member, IEEE, Yanbo Chen, Member, IEEE, Jin Ma, Member, IEEE, Yi Zhao, and Yuan-Ying Chi.

[29] A New Simplified Doubly Fed Induction Generator Model for Transient Stability Studies, IEEE TRANSACTIONS ON ENERGY CONVERSION, VOL. 30, NO. 3, September 2015. By Dong-Joon Kim, Member, IEEE, Young-Hwan Moon, Member, IEEE, and Hae-Kon Nam, Member, IEEE.

[30] Stochastic Transient Stability Analysis of Transmission Systems with Inclusion of Energy Storage Devices, IEEE TRANSACTIONS ON POWER SYSTEMS, VOL. 33, NO. 1, JANUARY 2018, by Alvaro Ortega, Student Member, IEEE, and Federico Milano, Fellow, IEEE.

[31] Real-Time Prediction and Control of Transient Stability Using Transient Energy Function, IEEE TRANSACTIONS ON POWER SYSTEMS, VOL. 32, NO. 2, MARCH 2017, Pratyasa Bhui and Nilanjan Senroy, Member, IEEE.

[32] An Automated Transient Stability Constrained Optimal Power Flow Based on Trajectory Sensitivity Analysis, IEEE TRANSACTIONS ON POWER SYSTEMS, VOL. 32, NO. 1, JANUARY 2017, Lei Tang, Member, IEEE, and Wei Sun, Member, IEEE.

[33] Coordinated Control of Optimized SFCL and SMEs for Improvement of Power System Transient Stability, IEEE TRANSACTIONS ON APPLIED SUPERCONDUCTIVITY, VOL. 22, NO. 3, June 2012, by Issarachai Ngamroo and Sitthidet Vachirasricirikul.

[34] Power Factor Corrected Zeta Converter Based Improved Power Quality Switched Mode Power Supply, IEEE TRANSACTIONS ON INDUSTRIAL ELECTRONICS, VOL. 62, NO. 9, SEPTEMBER 2015, by Shikha Singh, Student Member, IEEE, Bhim Singh, Fellow, IEEE, G. Bhuvaneswari, Senior Member, IEEE, and Vashist Bist, Member, IEEE.

[35] Very High-Frequency PWM Buck Converters Using Monolithic GaN Half-Bridge Power Stages with Integrated Gate Drivers, IEEE TRANSACTIONS ON POWER ELECTRONICS, VOL. 31, NO. 11, November 2016, by Yuanzhe Zhang, Student Member, IEEE, Miguel Rodr´ıguez, Member, IEEE, and Dragan Maksimovic´, Fellow, IEEE.

[36] Analytical Determination of Conduction and Switching Power Losses in Flying-Capacitor-Based Active Neutral-Point-Clamped Multilevel Converter, IEEE TRANSACTIONS ON POWER ELECTRONICS, VOL. 31, NO. 8, August 2016, by Arash Khoshkbar Sadigh,

Member, IEEE, Vahid Dargahi, Student Member, IEEE, and Keith A. Corzine, Senior Member, IEEE.

[37] Three-Phase Multilevel PWM Rectifiers Based on Conventional Bidirectional Converters, IEEE TRANSACTIONS ON POWER ELECTRONICS, VOL. 25, NO. 3, MARCH 2010, by Marcelo Lobo Heldwein, Member, IEEE, Samir Ahmad Mussa, Member, IEEE, and Ivo Barbi, Senior Member, IEEE.

[38] Extremely Sparse Parallel AC-Link Universal Power Converters, IEEE TRANSACTIONS ON INDUSTRY APPLICATIONS, VOL. 52, NO. 3, MAY/JUNE 2016, by S.A.KH. Mozaffari Niapour, Member, IEEE, and Mahshid Amirabadi, Member, IEEE.

[39] Comparison of the Modular Multilevel DC Converter and the Dual-Active Bridge Converter for Power Conversion in HVDC and MVDC Grids, IEEE TRANSACTIONS ON POWER ELECTRONICS, VOL. 30, NO. 1, JANUARY 2015, by Stefan P. Engel, Student Member, IEEE, Marco Stieneker, Student Member, IEEE, Nils Soltau, Student Member, IEEE, Sedigheh Rabiee, Student Member, IEEE, Hanno Stagge, Member, IEEE, and Rik W. De Doncker, Fellow, IEEE, (Special Issue on Modular Multilevel Converters, 2014).

[40] Direct Power Control of Series Converter of Unified Power-Flow Controller With Three-Level Neutral Point Clamped Converter, IEEE TRANSACTIONS ON POWER DELIVERY, VOL. 27, NO. 4, October 2012, by Jan Verveckken, Student Member, IEEE, Fernando Silva, Senior Member, IEEE, Dionísio Barros, Member, IEEE, and Johan Driesen, Senior Member, IEEE.

[41] A Single-Sensor-Based MPPT Controller for Wind-Driven Induction Generators Supplying DC Microgrid, IEEE TRANSACTIONS ON POWER ELECTRONICS, VOL. 31, NO. 2, February 2016, by V. Nayanar, N. Kumaresan, Member, IEEE, and N. Ammasai Gounden.

[42] Comparative Study of Wind Turbine Power Converters Based on Medium-Frequency AC-Link for Offshore DC-Grids, IEEE JOURNAL OF EMERGING AND SELECTED TOPICS IN POWER ELECTRONICS, VOL. 03, NO. 2, June 2015, by Rene Barrera-Cardenas and Marta Molinas, Member, IEEE.

[43] V2G Parking Lot with PV Rooftop for Capacity Enhancement of a Distribution System, IEEE TRANSACTIONS ON SUSTAINABLE ENERGY, VOL. 5, NO. 1, JANUARY 2014, Uwakwe C. Chukwu, Member, IEEE, and Satish M. Mahajan, Senior Member, IEEE.

[44] Single-Phase On-Board Bidirectional PEV Charger for V2G Reactive Power Operation, IEEE TRANSACTIONS ON SMART GRID, VOL. 6, NO. 2, MARCH 2015, by Mithat C. Kisacikoglu, Member, IEEE, Metin Kesler, Member, IEEE, and Leon M. Tolbert, Fellow, IEEE.

[45] Reactive Power Compensation Capabilities of V2G-Enabled Electric Vehicles, IEEE TRANSACTIONS ON POWER ELECTRONICS, VOL. 32, NO. 12, DECEMBER 2017, Giuseppe Buja, Life Fellow, IEEE, Manuele Bertoluzzo, and Christian Fontana, Member, IEEE.

[46] Effective Utilization of Available PEV Battery Capacity for Mitigation of Solar PV Impact and Grid Support with Integrated V2G Functionality, IEEE TRANSACTIONS ON SMART GRID, VOL. 7, NO. 3, MAY 2016, by M. J. E. Alam, Member, IEEE, Kashem M. Muttaqi, Senior Member, IEEE, and Danny Sutanto, Senior Member, IEEE

[47] Abnormality in power system transient stability control of BESS/STATCOM, The 6th International Conference on Renewable Power Generation (RPG) 19–20 October 2017, by Jun Liu1, Can Su1, Xu Wang1, Wanliang Fang1, Shuanbao Niu2, Lin Cheng2.

[48] Transient Stability and Voltage Regulation in Multimachine Power Systems Vis-à-Vis STATCOM and Battery Energy Storage, IEEE TRANSACTIONS ON POWER SYSTEMS, VOL. 30, NO. 5, September 2015, by Adirak Kanchanaharuthai, Member, IEEE, Vira Chankong, Senior Member, IEEE, and Kenneth A. Loparo, Fellow, IEEE.